



U.S. DRIVE Highlights of Technical Accomplishments 2012

March 2013



Preface

U.S. DRIVE (*Driving Research and Innovation for Vehicle efficiency and Energy sustainability*) is a voluntary government-industry partnership focused on precompetitive, advanced automotive and related infrastructure technology research and development (R&D). Partners are the United States Department of Energy (DOE); the United States Council for Automotive Research LLC (USCAR)—a consortium composed of Chrysler Group LLC, Ford Motor Company, and General Motors; Tesla Motors, Inc.; five energy companies—BP America, Chevron Corporation, Phillips 66 Company, ExxonMobil Corporation, and Shell Oil Products US; two electric utilities—DTE Energy and Southern California Edison; and the Electric Power Research Institute.

By providing a framework for frequent and regular interaction among technical experts in common areas of expertise, the Partnership accelerates technical progress, helps to avoid duplication of efforts, ensures that publicly funded research delivers high-value results, and overcomes high-risk barriers to technology commercialization.

U.S. DRIVE partners selected the technical highlights contained in this document from hundreds of DOE-funded projects conducted by some of the nation's top scientists and engineers. Each one-page summary represents what DOE and automotive, energy, and utility industry partners collectively consider to be significant progress in the development of advanced automotive and infrastructure technologies. This report is organized by technical area, with highlights in three general categories:

Vehicles

- Advanced Combustion and Emissions Control
- Electrical and Electronics
- Electrochemical Energy Storage
- Fuel Cells
- Materials
- Vehicle Systems and Analysis

Crosscutting

- Codes and Standards
- Onboard Hydrogen Storage
- Grid Interaction

Fuels

- Fuel Pathway Integration
- Hydrogen Delivery
- Hydrogen Production

More information about U.S. DRIVE, including prior year accomplishments reports, is available on the DOE (www.vehicles.energy.gov/about/partnerships/usdrive.html) and USCAR (www.uscar.org) websites.

Advanced automotive and energy infrastructure technologies are entering the market in increasing numbers, and technologies that were only concepts less than a decade ago are now approaching initial commercial readiness. These advancements are the result of partners working together to achieve a common goal. With continued progress resulting from the joint efforts of government, industry, and academic experts, U.S. DRIVE is helping to increase the competitiveness of American industry and secure U.S. leadership in an increasingly competitive global market to enable a clean and sustainable transportation energy future.

Note: Common abbreviations used through this report

AEV – All Electric Vehicle

ANL – Argonne National Laboratory

BNL – Brookhaven National Laboratory

EPA – Environmental Protection Agency

EDV – Electric Drive Vehicle

EUCAR – European Council for Automotive R&D

EV – Electric Vehicle

EVSE – Electric Vehicle Supply Equipment

DOE – Department of Energy

FCV – Fuel Cell Electric Vehicle

HEV – Hybrid Electric Vehicle

INL – Idaho National Laboratory

LANL – Los Alamos National Laboratory

Li-Ion – Lithium-Ion

NIST – National Institute of Standards and Technology

NREL – National Renewable Energy Laboratory

ORNL – Oak Ridge National Laboratory

PEV – Plug-In Electric Vehicle

PHEV – Plug-In Hybrid Electric Vehicle

PNNL – Pacific Northwest National Laboratory

SNL – Sandia National Laboratories

SRNL – Savannah River National Laboratory

USABC – United States Advanced Battery Consortium

USAMP – United States Automotive Materials Partnership

Table of Contents

Preface..... i

VEHICLE TECHNOLOGIES 1

Advanced Combustion and Emission Control..... 1

*Multi-Mode RCCI Engine Map Used to Demonstrate Potential Improvements
in Modeled Fuel Economy* 2

*Newly Developed Conceptual Model Describes In-Cylinder Processes
of Low-Temperature Combustion* 3

Gasoline Compression Ignition Demonstrated over a Significant Light-Duty Engine Operating Range 4

Surrogate Fuels Match Properties of Real-World Gasoline and Diesel Fuels 5

Gasoline with 20% Ethanol Extends High-Load Limit of HCCI to 20 Bar IMEP_g 6

In-Cylinder Mixture Formation Quantified for Low-Temperature, Light-Duty Diesel Combustion 7

*New Aging Protocol Enables More Rapid Laboratory Assessment of Useful Life
for Urea SCR/DOC Aftertreatment Systems* 8

*“Passive SCR” Demonstrates Lower-Cost Emission Control to Enable Fuel-Efficient
Lean Gasoline Engines* 9

Fuel Penalty Reduction of 50% Using Electrically Heated Diesel Particulate Filter Technology 10

Electrical and Electronics 11

Motor Efficiency Improvements 12

Improved High-Temperature Polymer Film Capacitor Fabrication 13

Electric Motor Thermal Management 14

*New Understanding of Alnico Magnets Helps Design Improvements to Boost Properties
for Drive Motors* 15

Electrochemical Energy Storage 16

High-Energy Lithium-Ion Batteries for EVs 17

GenII Prismatic Cell Development 18

EV Technology Assessment Program 19

A High, Specific-Energy PHEV Battery Pack with a Robust Thermal System 20

Scale-Up and Production of Low-Cost Nickel/Manganese/Cobalt Cathode Material 21

Modeling and Understanding Lithium-Ion Battery Performance and Cost 22

Computer-Aided Analysis Methods for Lithium-Ion Battery Design Developed and Deployed 23

Cell Fabrication Using Advanced Battery Materials 24

AutoLion™: A Thermally Coupled Lithium-Ion Battery Model 25

<i>Investigation and Improvement of High-Voltage Cathode Material</i>	26
<i>A New Synthesis Approach to High-Energy Manganese Rich Cathodes</i>	27
<i>Lithium-Ion Electrolytes with Wide Operating Temperature Ranges</i>	28
<i>Scale-Up of Promising Overcharge Shuttle for Industry Evaluation</i>	29
<i>High-Capacity Hollow Silicon Nanofiber Anodes</i>	30
<i>Single Crystal Diagnostics Leads to Improved Material Performance</i>	31
<i>Technologies for Improved Safety of Lithium-Ion Batteries</i>	32
<i>Use of Atomic Layer Deposition Coatings to Stabilize High-Voltage, High-Energy Cathode Materials</i>	33
Fuel Cells	34
<i>Model Validates Performance and Cost Projections</i>	35
<i>Model Prediction of Performance for Low Platinum Use</i>	36
<i>Designing Durable Fuel Cell Catalysts</i>	37
<i>Investigation of Micro- and Macro-Scale Transport Processes for Improved Fuel Cell Performance</i>	38
<i>Novel Non-Platinum Group Metal Electrocatalysts for Fuel Cell Applications Synthesized</i>	39
Materials	40
<i>Optimization of High-Volume Warm Forming For Lightweight Sheet Alloys</i>	41
<i>Integrated Computational Materials Engineering of Magnesium</i>	42
<i>Magnesium Front-End Research and Development</i>	43
<i>Establishment of Quality Mapping for Ductility in Magnesium Casting</i>	44
<i>Non-Rare Earth Containing Wrought Magnesium Development</i>	45
<i>Advanced Plasma Oxidation</i>	46
Vehicle Systems and Analysis	47
<i>New Air Conditioning Model Validated and Released</i>	48
<i>Accelerating EV Development with New Test Standards</i>	49
<i>Vehicle Mass: Road Load and Energy Consumption Impact</i>	50
<i>Wireless Power Transfer: Stationary Charging</i>	51
CROSSCUTTING TECHNOLOGIES	52
Codes and Standards	52
<i>Optimizing Materials Testing for Hydrogen Service</i>	53
<i>Publication of Harmonized SAE J2719 Hydrogen Fuel Quality for Fuel Cell Vehicles</i>	54

Onboard Hydrogen Storage	55
<i>Material Requirements for Viable Onboard Hydrogen Storage Using Metal Hydrides</i>	56
<i>Systematic Analysis and Avoidance of Material-Based Hydrogen Storage System Failure Modes</i>	57
<i>Best Practices Reference Document Released</i>	58
<i>Validation of Hydrogen Storage Using Weak Chemisorption</i>	59
Grid Interaction	60
<i>Enabling Technologies for Vehicle-Grid Communication</i>	61
FUEL INFRASTRUCTURE TECHNOLOGIES	62
Fuel Pathway Integration	62
<i>Well-to-Wheel Analysis</i>	63
Hydrogen Delivery	64
<i>Increased Tube Trailer Capacity</i>	65
Hydrogen Production	66
<i>Improved Hydrogen Evolution in Recombinant Cyanobacteria</i>	67
<i>Updates to the Hydrogen Production Analysis Model</i>	68

VEHICLE TECHNOLOGIES



Multi-Mode RCCI Engine Map Used to Demonstrate Potential Improvements in Modeled Fuel Economy

Drive cycle simulations of multi-mode RCCI combustion demonstrate greater than 15% drive cycle fuel economy improvement compared to a gasoline engine baseline.

Argonne National Laboratory

Reactivity controlled compression ignition (RCCI) combustion makes use of in-cylinder blending of two fuels with differing reactivity to tailor the reactivity of the fuel charge for improved control of the combustion process. This allows stable, low-temperature combustion to be extended over more of the light-duty drive cycle load range. RCCI's potential to reduce drive cycle fuel economy and emissions is not clearly understood. ORNL investigated its potential by simulating the fuel economy and emissions for a multi-mode RCCI-enabled vehicle operating over a variety of U.S. drive cycles in a first-of-its-kind study. The approach used a vehicle simulation with experimental engine maps compared to a 2009 port-fuel injected (PFI) gasoline engine in the same vehicle—a midsize sedan with an automatic transmission.

An experimental RCCI engine map was developed on a four-cylinder 1.9L diesel engine that was modified for port-fuel injection and pistons designed for RCCI operation. Certification-grade gasoline and a 20% biodiesel blend fuel were used for the engine map, which expanded RCCI operation compared to using ultra-low sulfur diesel fuel. The peak efficiency from the RCCI operating map was found to be within the region that is relevant to the federal light-duty drive cycles, unlike conventional diesel combustion whose peak efficiency is well outside the drive cycle. However, the current range of the experimental RCCI engine map does not allow full coverage of many light-duty drive cycles. A multi-mode RCCI strategy was employed where the engine switches from RCCI to conventional diesel combustion (CDC) when demanded speed and load fall outside of the RCCI range of this map.

Multi-mode RCCI operation was found to increase drive cycle fuel economy by at least 15% compared to the modeled PFI baseline over all hot drive cycles examined (no warm-up portion). Increased efficiency with RCCI over much of the map allowed for increased fuel economy. Engine-out drive cycle emissions were compared to CDC operation over the full load-speed range—it was found to offer at least a 20% decrease in nitrogen oxide emissions on both city and highway driving cycles. However, hydrocarbon (HC) and carbon monoxide (CO) emissions increased with RCCI on the order of two to three times compared to CDC. The increased HC and CO emissions, along with reduced exhaust temperatures, will be a challenge for exhaust aftertreatments.

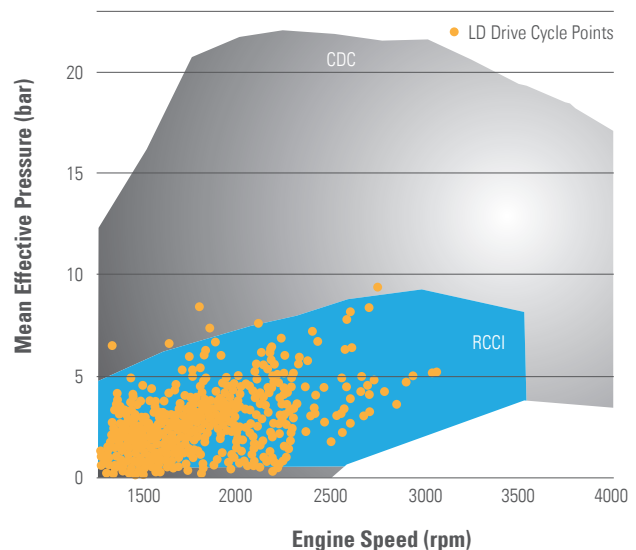


Figure 1. RCCI portion of multi-mode engine operating map shown with light-duty (LD) “city” drive cycle speed and load points overlain.

Newly Developed Conceptual Model Describes In-Cylinder Processes of Low-Temperature Combustion

After years of optical engine experiments and computer modeling, the widely used diesel conceptual model is expanded to show in-cylinder mixing, combustion, and emissions for low-temperature diesel combustion.

Sandia National Laboratories

Over one decade ago, laser and optical diagnostic data led to a conceptual model for diesel combustion (left column below). This model served as a foundation of understanding across industry and academia. However, it does not cover the advanced combustion strategies now being considered for enabling higher-efficiency, cleaner engines. These new, low-temperature combustion (LTC) strategies are very different, and the model needs to be expanded to cover them.

Based on recent optical engine research and computer modeling, a new conceptual model has been proposed for LTC processes. In the prior diesel model, insufficiently mixed fuel generated soot and smoke (red),

and a hot flame (green) formed nitrogen oxides (NO_x), a smog precursor. By contrast, exhaust-gas recirculation (EGR) and modified fuel injection in LTC engines for both trucks (middle) and cars (right) delays fuel ignition until after the end of fuel injection. This ensures that the fuel is better mixed with air, and that much less soot is formed. The EGR also reduces temperatures (by definition, LTC), which reduces both soot and NO_x formation. The data also show that incomplete combustion (purple/gray) arises from over-mixed regions, which provides guidance for optimization to reduce carbon monoxide (CO) and unburned hydrocarbon (UHC) emissions for LTC.

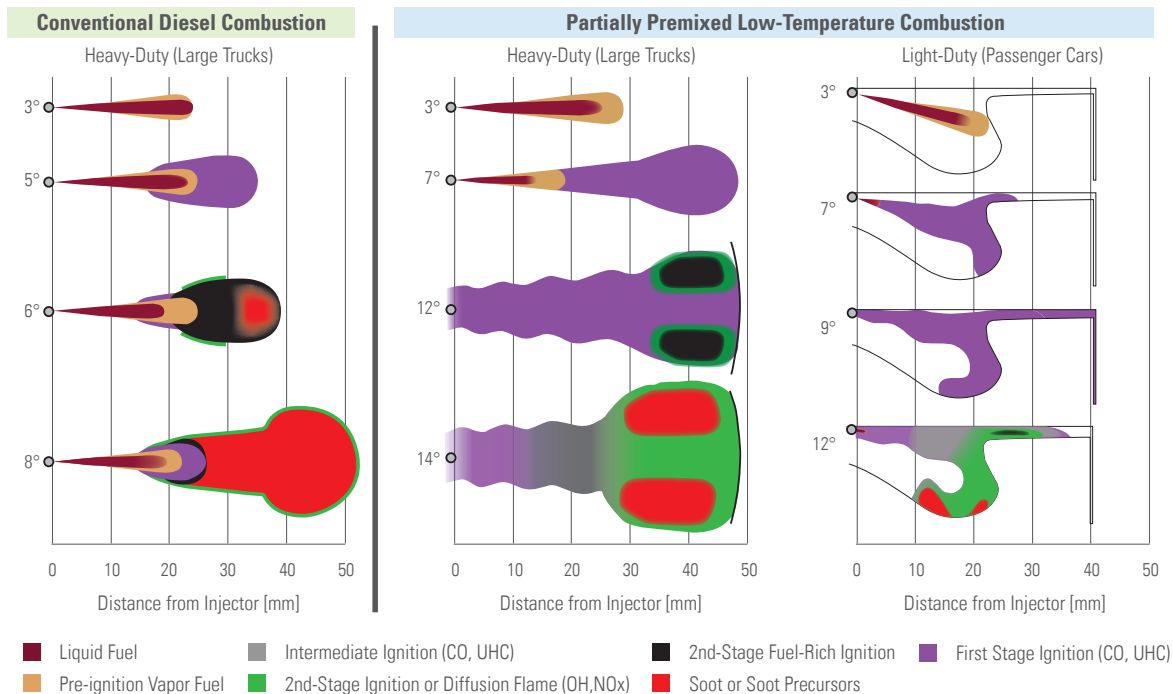


Figure 1. Conceptual model features for conventional heavy-duty diesel combustion (left) with partially premixed, low-temperature diesel combustion for either heavy-duty trucks (middle) or light-duty passenger cars (right).

Gasoline Compression Ignition Demonstrated over a Significant Light-Duty Engine Operating Range

High efficiency with low NO_x and particulate emissions were obtained over the majority of the engine map using direct injection gasoline compression ignition.

University of Wisconsin—Madison and General Motors

Guided by simulation and refined by experiments, high-efficiency and low-emission gasoline compression ignition (GCI) combustion has been demonstrated over a substantial portion of the light-duty operating range. Successful compression ignition of gasoline/air/exhaust-gas mixtures was controlled through multiple injections and variation of injection pressure, oxygen concentration, and boost pressure. Engine operation from 1,500–2,500 RPM, with load ranging from 3–16 bar brake mean effective pressure (BMEP), was achieved (Figure 1). Acceptable operation was constrained to have maximum rates of pressure rise less than 10 bar per degree crank angle. Emissions met EPA 2010 light-duty particulate matter (PM) and nitrogen oxide (NO_x) standards, with NO_x emissions always less than 1 g/kg-fuel, and PM significantly less than 0.1 g/kg-fuel. The gross indicated specific fuel consumption (gISFC) ranged between 175–190 g/kW-hr, which is comparable to conventional diesel combustion and diesel low-temperature combustion (LTC) (Figure 1). At the 16 bar BMEP operating point, the gross indicated thermal efficiency was more than 47%.

Figure 1 shows the extent of the GCI operating regime achieved to date superimposed on the operating map of the base diesel engine. The color contours show the fuel consumption (gISFC). The bar chart compares GCI fuel consumption and emissions to diesel LTC, conventional diesel, and spark-ignited direct injection (SIDI) gasoline. Although GCI has higher hydrocarbon (HC) and carbon monoxide (CO) emissions than conventional diesel or SIDI (as is typical of low-temperature combustion modes), GCI has fuel consumption comparable to a conventional diesel with much lower NO_x and particulate emissions.

Optimal injection pressures were found for GCI as speed and load are varied. High load used triple injection: the first injection establishes a premixed base charge, the second controls the start of combustion, and the third tailors the load.

Reducing HC and CO emissions and maintaining stable combustion during inlet-temperature perturbations are now being addressed. Results demonstrate that fueling rate and injection control can be used to counter the impact of intake temperature fluctuations on combustion quality in the mid-load operating regime.

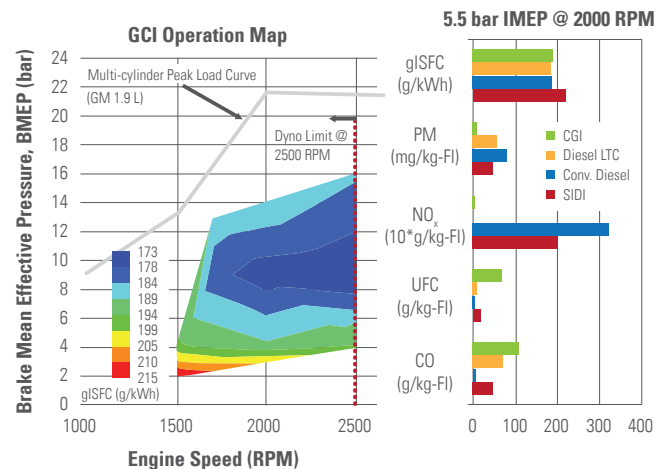


Figure 1. GCI operating map with fuel consumption (gISFC) contours (left) and comparison of fuel consumption and emissions with other combustion modes (right). Diesel LTC is analogous to GCI, but using diesel fuel with very high EGR rates. SIDI refers to a current spark-ignition direct injection gasoline engine.

Surrogate Fuels Match Properties of Real-World Gasoline and Diesel Fuels

Chemically simplified “surrogate” fuels with five to eight components match the chemical structure, ignition, and volatility of real-world fuels and enable computational studies of advanced combustion strategies.

Lawrence Livermore National Laboratory and Sandia National Laboratories

Working with researchers from engine manufacturers, energy companies, and other U.S. national and Canadian federal laboratories, techniques were developed to create surrogate fuels that have performance characteristics similar to those of more complex, real-world fuels, while containing only a small number of chemical compounds (see Figure 1). This chemical simplification is a key step toward the accurate numerical simulation of spray, mixing, and combustion processes for realistic fuels. Surrogate fuels also are valuable experimentally because they can provide data for model development and validation in which all engine and fuel parameters are well characterized and controlled.

For gasoline fuels, a new approach was developed to match the octane and compositional characteristics of real gasoline fuels. The gasoline surrogate developed using this approach matched the ignition characteristics of a real-world gasoline in a rapid compression machine and a shock tube; it also matched the pre-ignition heat release profiles in a homogeneous-charge compression-ignition engine. Working under the auspices of Coordinating Research Council Project AVFL-18, diesel surrogates were formulated to match carbon-bond types, ignition qualities, and volatility characteristics of real-world fuels within 5 mol%, 4%, and 2%, respectively, on average. Novel aspects of the approach for diesel fuels include applying nuclear magnetic resonance spectroscopy techniques and the advanced distillation curve to characterize carbon-bond types and volatility, respectively.

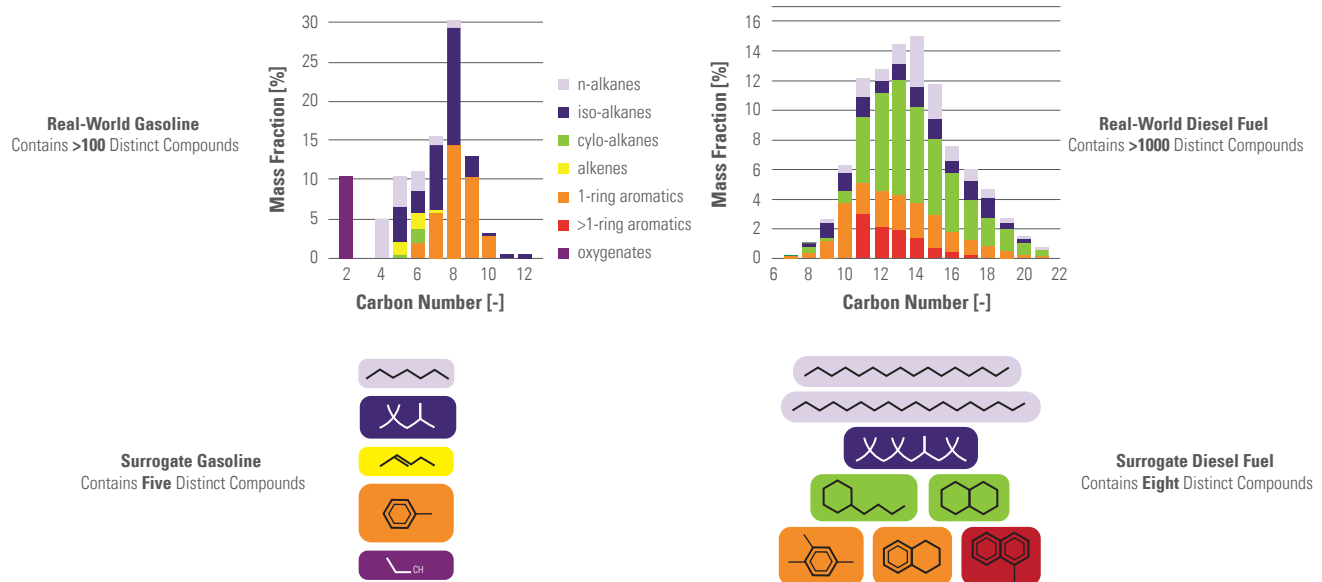


Figure 1. Highly simplified, yet still accurate, surrogate gasoline and diesel fuels have been developed.

Gasoline with 20% Ethanol Extends High-Load Limit of HCCI to 20 Bar IMEP_g

Boosted HCCI engines fueled with regular 87-octane gasoline and 10% or 20% ethanol achieve loads similar to conventional turbo-charged diesel engines, with NO_x less than 0.02 g/kWh and undetectable soot.

Sandia National Laboratories

Responding to the need to reduce petroleum consumption, gasoline in the United States commonly contains up to 10% ethanol (E10). Efforts to raise this to 15% and 20% levels (E20) are being considered. Petroleum consumption can also be reduced by improving engine efficiency. Homogeneous-charge compression-ignition (HCCI) engines and partially stratified variants of HCCI align with this goal because they have high efficiencies with very low nitrogen oxide and soot emissions.

Adding ethanol changes the auto-ignition characteristics of gasoline, and it is important to understand how this affects the performance of HCCI engines. Of particular significance is the effect of ethanol on performance with intake-pressure boost, which substantially increases the load range and can also improve efficiency.

The performance of conventional gasoline (E0), E10, and E20 for HCCI combustion was compared at both naturally aspirated and boosted conditions. Experiments were conducted in a medium-duty, single-cylinder research engine with a displacement of 0.98L at 1,200 RPM. The E10 and E20 were obtained by blending pure ethanol with a standard petroleum-based gasoline, having an antiknock index (AKI) of 87. This approach eliminates variations in performance due to changes in the composition of the base gasoline, although the AKI is increased.

Figure 1 shows the maximum load that could be attained for intake pressures from naturally aspirated (1 bar) to the maximum allowable boost with exhaust-gas recirculation (EGR) and several ethanol levels. For all points, maximum pressure-rise rates were limited to prevent engine knock and to avoid cylinder-head structural issues.

In addition to allowing higher loads, intake boost enhances autoignition. Compensating by intake-temperature reduction alone limits the load increase to 8.8 bar gross indicated mean effective pressure (IMEP_g). Further compensation by using EGR to reduce compressed-gas temperatures and oxygen concentrations allows loads up to 16.3 bar IMEP_g with E0. At this point, the load is limited by a lack of oxygen due to the amount of EGR required to prevent overly advanced auto-ignition. Increasing the ethanol content reduces the EGR required at high boost, leaving more air available for combustion and high-load limits of 18.1 and 20.0 bar IMEP_g for E10 and E20, respectively. The results demonstrate that HCCI can achieve diesel-like loads.

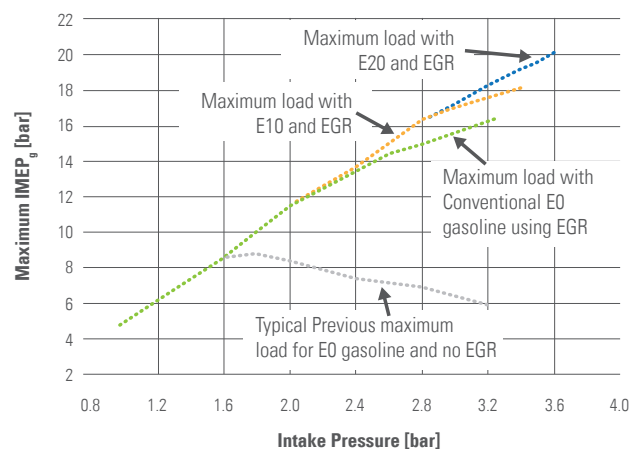


Figure 1. Maximum load (IMEP_g) as a function of intake boost for fully premixed HCCI at 1,200 RPM with E0, E10, and E20 gasoline. All boosted data points have no engine knock, undetectable soot, and NO_x < 0.02 g/kWh, which represents a Tier 2, Bin 2 emissions value.

In-Cylinder Mixture Formation Quantified for Low-Temperature, Light-Duty Diesel Combustion

Proper formation of the combustible mixture is the key to high efficiency and low HC and CO emissions.

Sandia National Laboratories—Combustion Research Facility

Advanced, low-temperature diesel combustion is widely recognized as having the potential to provide very low engine-out particulate and nitrogen oxide emissions. However, attendant low-compression ratios and high exhaust-gas recirculation rates can lead to efficiency loss and accompanying high hydrocarbon (HC) and carbon monoxide (CO) emissions—especially at the low loads that dominate urban drive cycles. In order to realize the full potential of these combustion systems, the mixture preparation process must be carefully controlled to avoid the formation of both overly fuel-lean and overly fuel-rich regions.

Laser-induced fluorescence from fuel molecules was used to make quantitative measurements of the in-cylinder fuel-air equivalence ratio distribution in a light-duty engine. Although numerous mixture preparation studies have been performed in heavy-duty diesel engines or large combustion vessels, quantitative measurements of mixture formation in light-duty engines, where wall interactions and strong swirl are significant, have not previously been obtained.

The figure below shows sample results obtained in three horizontal planes at the start of the high-temperature heat release. The measured equivalence

ratio distributions clearly illustrate potential sources of HC and CO:

- In the squish volume (left image), the fuel jets have penetrated nearly to the cylinder wall—such that gas expansion due to combustion will likely force fuel into the ring-land crevice.
- Despite nearly 15° of ignition delay, fuel-rich mixture persists within the squish volume.
- In the central regions of the clearance/squish volume and bowl rim planes (left and center images), there is a large quantity of over-lean mixture that will not oxidize completely. Our previous work has shown that such mixture is the dominant source of HC and CO emissions.
- Mixture in the lower bowl is found to burn completely and contribute little to engine-out HC and CO (right image).

These measurements improve understanding of the mixture formation process and provide quantitative data for developing and validating predictive engine design and simulation tools.

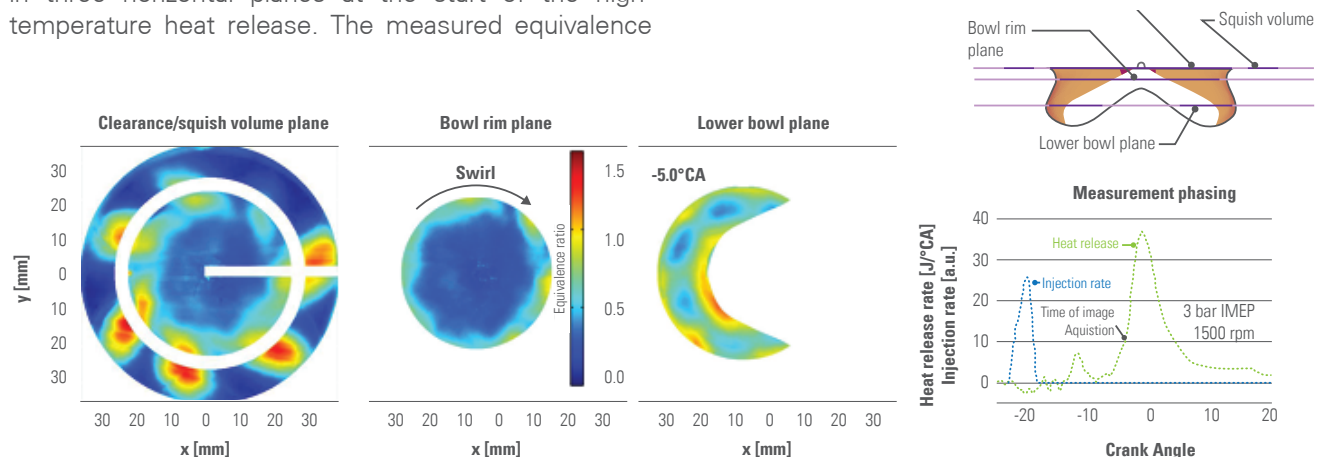


Figure 1. Measured fuel-air equivalence ratio distributions at the start of high-temperature heat release for a light-load, early-injection, partially premixed operating condition.

New Aging Protocol Enables More Rapid Laboratory Assessment of Useful Life for Urea SCR/DOC Aftertreatment Systems

Laboratory-aged SCR catalyst duplicates the Nitrogen Oxides (NO_x) conversion of a vehicle-aged catalyst. The new protocol and catalyst-deactivation understanding have potential to reduce development time and cost.

Pacific Northwest National Laboratory and General Motors

Diesel engines offer substantially higher fuel efficiency, excellent driving performance, and reduced carbon dioxide emissions compared to stoichiometric gasoline engines. However, meeting the stringent emission standards with affordable methods has been a major challenge. The selective catalytic reduction (SCR) of nitrogen oxides (NO_x) by urea (urea-SCR) is one of the more promising technologies for NO_x emission control for diesel engine exhausts.

To ensure successful commercialization of the urea-SCR technology, high catalytic activity and durability for the life of the vehicle are critical for the emission control system. Because the use of this technology for light-duty diesel vehicle applications is new, the relative lack of experience makes it especially challenging to satisfy durability requirements. Of particular concern is being able to realistically simulate actual field aging of the catalyst systems under laboratory conditions.

Fresh, laboratory-aged and vehicle-aged Diesel Oxidation Catalyst (DOC) and SCR catalysts were investigated to better understand the various aging factors that impact the long-term performance of catalysts. The result is a new protocol for catalyst aging in a laboratory that matches the NO_x conversion of a vehicle-aged catalyst (Figure 1). In addition, by varying laboratory aging time and temperature with a considerable number of catalyst samples, the operational limits to avoid catalyst deactivation were determined. In the DOC, deactivation is due to growth and alloying of the precious metal. For the urea-SCR, deactivation is due to collapse of the zeolite structure and growth of active metal par-

ticles with reduced surface area. A rapid catalyst-aging protocol and understanding of the catalyst deactivation process have potential to reduce development time and cost.

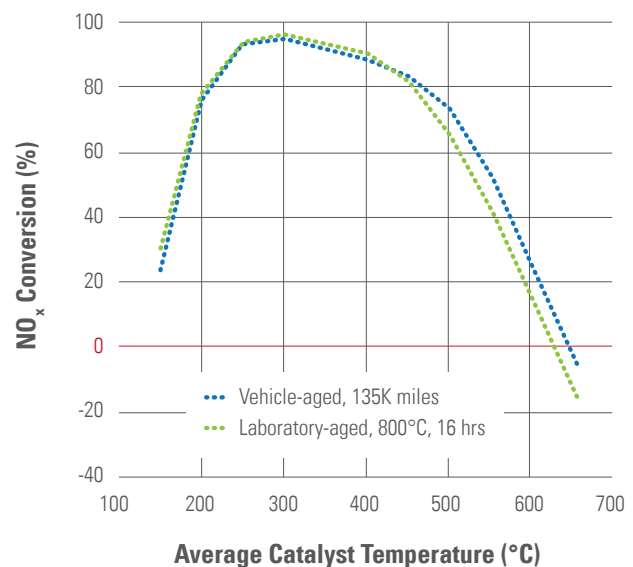


Figure 1. NO_x conversion results over a middle core of the 135,000-mile vehicle-aged copper-zeolite SCR catalyst and the SCR catalyst reactor-aged at 800°C for 16 hours. NO_x conversion was measured with 200 ppm NO and 200 ppm NH₃ input.

“Passive SCR” Demonstrates Lower-Cost Emission Control to Enable Fuel-Efficient Lean Gasoline Engines

More than 99% of NO_x emissions in simulated exhaust reduced using existing three-way catalyst in combination with a SCR catalyst without urea addition system.

Oak Ridge National Laboratory

Lean operation is a pathway to improve fuel economy for gasoline vehicles in the United States. One major barrier includes the reduction of nitrogen oxide (NO_x) in the oxygen-rich lean engine exhaust. Compared to lean-exhaust diesel vehicles that meet the stringent 2010 emissions standards, gasoline-based systems are challenged by higher exhaust temperature and higher engine-out NO_x emissions.

A potential approach to meet the emission standards for lean gasoline engines demonstrated by General Motors (GM) is a three-way catalyst (TWC) for onboard ammonia (NH_3) generation followed by a zeolite-based selective catalyst reduction (SCR) catalyst that uses the NH_3 to reduce the NO_x . ORNL evaluated this “passive SCR” concept for a wide range of catalyst materials and temperatures to improve understanding for its feasibility. Umicore and GM supplied catalysts and guidance for the project.

Using mainly bench reactor measurements, ORNL demonstrated 90%–100% conversion of engine produced NO_x to NH_3 over the TWC for a wide range of air-to-fuel ratios (AFRs) and temperatures. The conditions include a cycling AFR varying between mildly rich (AFR~14) and lean (AFR~24) conditions. For these conditions, the NO_x produced by the engine under lean conditions is substantially lower than the NO_x produced during mildly rich conditions by a factor of approximately 2. By controlling the operating temperature, AFR and cycle times greater than 99.5% of the overall NO_x produced can be removed.

The effects of TWC catalyst materials were evaluated. For higher temperatures (up to 550°C–660°C under appropriate AFR), Pd-only TWC formulations had superior NH_3 production efficiencies. For lower temperature

ranges (300°C–350°C), TWC formulations with NO_x storage components (similar to Lean NO_x Trap catalyst technology consisting of Pt, Pd, Rh, and alkaline earth metals) provided much greater NH_3 production.

The onboard NH_3 production technique can eliminate the costs and complexity of NH_3 delivery via urea systems. Currently, urea (a solution that converts to NH_3 when injected into the hot exhaust) is added to the exhaust and delivered to the SCR catalyst; however, costs for the urea tank, injector, control system, and temperature management are significant.

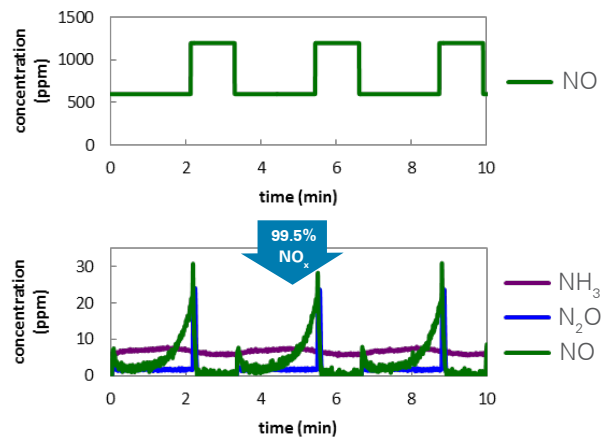


Figure 1. Passive SCR system inlet and outlet concentrations. NO_x is converted to NH_3 over a TWC (450°C inlet) under mildly rich conditions (AFR ~14), and the NH_3 is stored on an under-floor zeolite SCR catalyst (300°C). During fuel-efficient lean operation (AFR~24), NO_x is reduced by the stored NH_3 in the SCR catalyst. More than 99.5% NO_x conversion has been shown with this technique.

Fuel Penalty Reduction of 50% Using Electrically Heated Diesel Particulate Filter Technology

A combination of electrical heating and fuel addition heats and controls the temperature for soot oxidation during regeneration of a DPF.

General Motors, HRL Laboratories, and Oak Ridge National Laboratory

A technology developed by General Motors and HRL Laboratories—called Electrically Assisted Diesel Particulate Filter (EADPF)—uses a combination of fuel addition by in-cylinder injection and electrical heating to heat and control the temperature for soot oxidation during regeneration of a Diesel Particulate Filter (DPF). Studies at ORNL that used a 1.9L diesel engine demonstrated a 50% reduction in the fuel penalty and a 60% reduction in the regeneration time compared to DPF regeneration with only fuel. Both changes are significant for light-duty applications with low exhaust temperatures and shorter trip times.

In addition to the fuel penalty measurement, ORNL measured substrate temperatures during the regeneration process and studied the mechanical properties of the EADPF cordierite substrate. These data improve understanding of the regeneration process and potential for material failure.

To measure substrate temperatures, ORNL developed a fiber-optic-based technique based on blackbody radiation. Optical fibers with angled tips were inserted into the DPF channels at several locations to collect light emitted from the hot substrate during regeneration. The light spectra collected were analyzed to determine the substrate temperature. Results confirmed that oxidation occurred as a self-sustaining thermal wave along the flow axis and showed that peak substrate temperatures were highly dependent on soot loading prior to regeneration. Electrical heating initiated the thermal wave and allowed greater control of the process, thereby shortening the time and reducing the fuel quantity required to sustain DPF temperatures suitable for soot oxidation.

DPF thermal durability is an issue. Using a combination of modeling and experimental techniques, the ORNL team measured material properties of the DPF cordierite substrate. The substrate's elastic modulus was a factor

of 5 to 10 lower than literature values. Model predictions based on these more accurate measurements showed much greater durability and suggest that potential for DPF failure during regeneration is reduced.

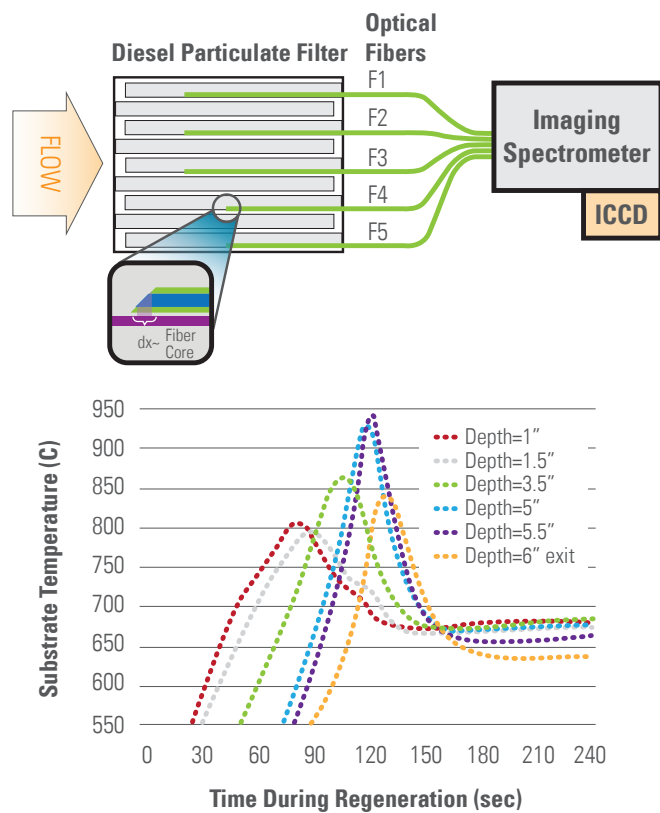


Figure 1. Schematic of fiber-optic-based substrate temperature measurement technique (above) and resulting data (below) showing thermal wave due to exothermic release from soot oxidation.

Electrical and Electronics



Motor Efficiency Improvements

Material developments in motor laminations and potting compounds result in heat reduction improvements of 18%, increased drive system efficiency of 2%, higher reliability, and lower costs.

Oak Ridge National Laboratory

Traction motors employed in hybrid, plug-in electric vehicles (PEV) and all electric vehicles (AEV) are predominantly interior permanent magnet (IPM) motors that are now too expensive due to rare earth magnet content. This project is focused on the development of magnetic and thermal materials to improve efficiency and reduce cost of traction drive motors for PEVs and AEVs.

Studies have been conducted at ORNL on conventional and grain-oriented electrical steel (GOES) laminations for higher-efficiency operation, as well as thermal-conducting epoxies for enhanced and more uniform heat dissipation in the motor windings.

The benefits of GOES for electric traction motors are best realized if the stator teeth are fabricated using radially oriented steel, and if the back iron is made using circumferentially oriented steel. A processing technique suitable for the manufacture of such lamination steel has been developed by ORNL for future deployment.

Core losses of representative lamination steels were obtained during the study, and three experimental stators were fabricated. Two stators were made using conventional material, one of which was potted using a Cotronics epoxy molding compound with thermal conductivity of approximately 3.2 W/m-K. A third stator was fabricated from a high silicon content steel (JFE 0.1 mm Super E-core 10JNEX900 material). The test stators are shown in Figure 1, and Table 1 details temperatures reached during testing. Figure 2 shows comparisons relative to a mass-produced, ORNL-benchmarked, best-in-class IPM stator.

Results confirm 22% lower peak temperature, more uniform temperature, and 18% lower heat rejection to the thermal management system.

Lessons learned on methods and materials to optimize efficiency for traction motors will be carried forward in future motor research and development efforts.

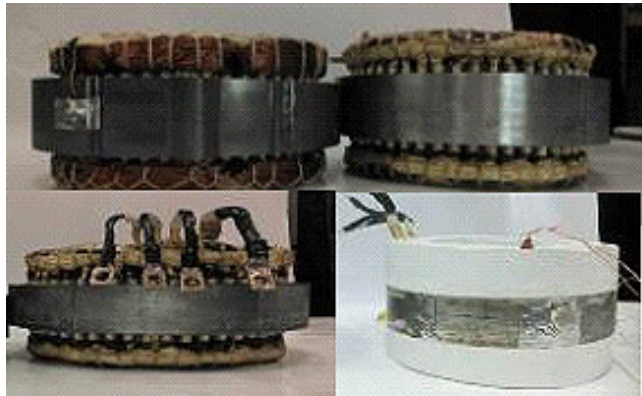


Figure 1. Stators fabricated for thermal and performance comparisons.

T (°C)	Baseline	29M19	Potted	JFE
Bore	115	108.7	94.49	97.7
On Diameter	116.36	106	95.78	99.87

Table 1. Steady State Temperature Comparison (t~20,000s) stator bore, on diameter and end turns

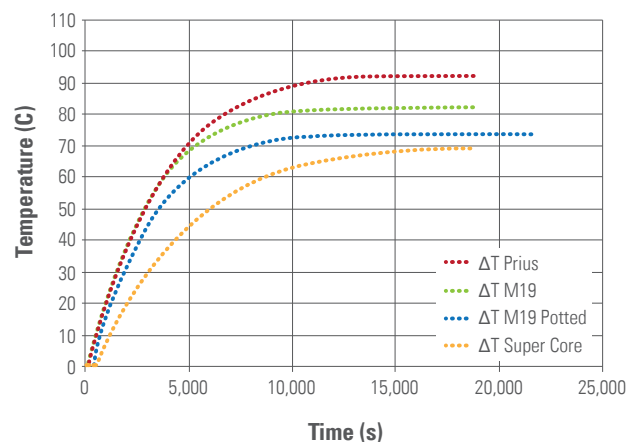


Figure 2. Loss reduction benefits of the experimental stators compared with that of a baseline motor.

Improved High-Temperature Polymer Film Capacitor Fabrication

Demonstration of inexpensive, extruded, high-temperature polymer film is a key milestone toward the development of lighter, smaller, less expensive inverters with improved reliability.

Sandia National Laboratories

Capacitors with thin polymer dielectrics are used within the inverter to absorb ripple current. The direct current (DC) bus capacitor presents significant barriers to meeting the U.S. DRIVE targets for cost, volume, reliability, and weight for future inverters. Currently, the DC bus capacitor contributes up to 23% of the cost and weight of an inverter, and up to 30% of an inverter's volume. Furthermore, inexpensive, commercially available polymer thin-film capacitors are limited by an operational temperature maximum of no greater than 120°C.

SNL recently developed a novel polymer dielectric material that is being used to create inexpensive (dielectric materials price less than \$0.02/μF), high-temperature polymer thin-film capacitors with increased energy densities for use in HEV inverters that could operate at elevated temperature environments and thus support the introduction of 105°C engine coolant cooled inverters.

In fiscal year 2012, SNL demonstrated the extrusion of the thin polymer dielectric film with thicknesses as thin as 3 μm. The ability to extrude the dielectric greatly reduces the production cost of capacitors. The team at SNL has demonstrated the production of approximately 100 m length roll of extruded polymer, which is currently being evaluated for the production of inexpensive, high-temperature capacitors. Prototype capacitors with both potting and tin alloy thermal spray deposited end termination contacts have been fabricated using the SNL-developed high-temperature polymer. Work is ongoing to identify the optimal plasticizer, which will minimize defects during the extrusion process and improve capacitor reliability.

The projected benefits include increased inverter reliability and improved capacitors, which can handle larger ripple currents as a result of the high-temperature dielectric materials.

	SNL High-Temperature Capacitors	Commercially Available Polyester Capacitors
Operational Temperature	>150°C	125°C
Material Cost/g	\$0.18	\$0.25
Energy Density	1.5-2.0 J/cm ³	1-1.5 J/cm ³

Table 1. Comparison of SNL high-temperature capacitors and commercially available polyester capacitors.

SNL has been developing the high-temperature dielectric material in collaboration with Electronic Concepts Inc. as the technology is transitioned from laboratory scale to production scale.

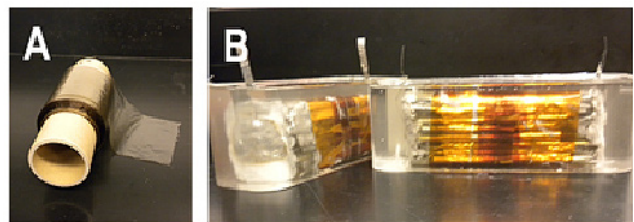


Figure 1. A) An image of the ~100 m roll of high-temperature dielectric, and B) packaged high-temperature capacitors.

Electric Motor Thermal Management

Thermal sensitivity analysis of multiple motor designs highlights and identifies critical areas to improve power capabilities of electric motors and shows that there is room to increase motor power density up to 100% through improved motor heat transfer.

National Renewable Energy Laboratory

In conjunction with ORNL and the University of Wisconsin–Madison, NREL completed a thermal sensitivity analysis across multiple motor designs to highlight and identify critical areas for improved thermal management of electric motors for future traction drive systems. Improved thermal management can improve motor power output and help reduce size and cost.

As the trend to electrify vehicle propulsion systems increases, the impact of thermal management on the electric motor will increase as the need for higher continuous power operation increases. The thermal management of electric motors depends on both the convective cooling applied to the motor and the internal passive thermal stack. The passive thermal stack consists of multiple elements and thermal interfaces, as shown in Figure 1.

NREL measured the thermal conductivity, specific heat, and contact resistances for motor steel laminations in the stator and rotor. The information supported a parametric finite element thermal sensitivity analysis for multiple motor configurations.

The analysis highlighted the impact of cooling on motor performance, as well as the areas for focused research improvements.

Improvements in convective cooling enable close to a doubling of motor power, with respect to the baseline, before the benefits diminish (Figure 2). As the convective cooling improves, the passive thermal stack materials and interfaces limit continued improvements in motor power. The passive thermal stack sensitivity study (Figure 3) shows the impact of operating condition on critical heat paths. Removing heat from the rotor is important at high operating speeds (A), while high torque operation is impacted by stator cooling (B).

Future work on this project will focus on convective heat transfer characterization of oil sprays/jets, as well as the impacts on winding insulation. The work has led to interactions with industry on the impacts of thermal management, temperature distributions, and methods for improved cooling. The work also supports future traction drive systems that utilize higher speed and motor designs with longer axial length.

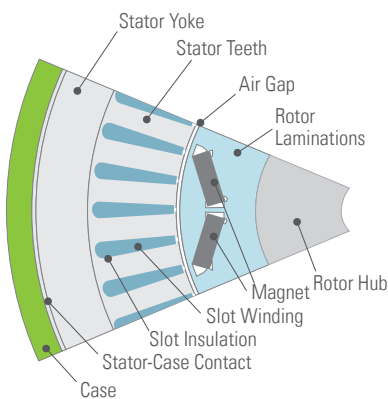


Figure 1. Elements of passive thermal stack of an electric motor.

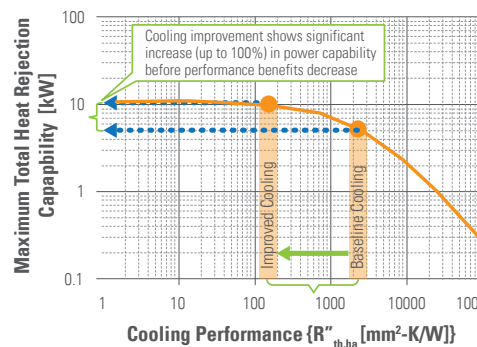


Figure 2. Potential for improved convective cooling to improve motor power capability.

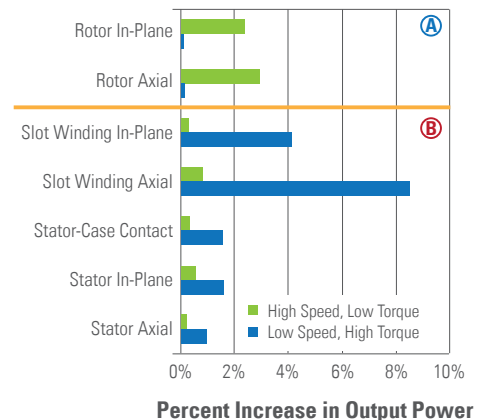


Figure 3. Percent improvement in motor output power when the highlighted element's (y-axis) thermal conductivity increases by 20%.

New Understanding of Alnico Magnets Helps Design Improvements to Boost Properties for Drive Motors

Atomic-scale characterization and theoretical analysis provide clues about how rare-earth-free alnico magnets can be improved for drive motor use with changes in processing and alloy design.

Ames Laboratory

Alnico magnets have been selected as the best near-term candidate to replace rare earth (RE) magnets in permanent magnet (PM) motors for HEV and PHEV drive systems. While these aluminum-nickel-cobalt-iron (Al-Ni-Co-Fe) PM alloys have been used widely since the 1940s, their development was “on hold” for about 40 years; displaced by superior RE magnets, especially neodymium-iron-boron (Nd-Fe-B), which have a five times energy product (MGOe) advantage at room temperature. However, for traction motors, wind power generation, and other elevated temperature uses (above 180°C), Nd-Fe-B has only a 20 MGOe versus 10 MGOe margin over the best alnico (type 9), which also has many advantages over Nd-Fe-B, including superior corrosion resistance and broadly available alloy constituents; although, Co costs are relatively high.

Alnico magnets that can match Nd-Fe-B at motor temperatures will require increased resistance to field reversals, yet there is scant understanding of these “coercivity” mechanisms for alnico magnets, beyond a preference for high content of magnetic Fe-Co (bcc) “bricks” that are highly elongated for “shape anisotropy” in a non-magnetic “mortar” (matrix). Our new study uses modern atomic-scale characterization on three types of commercial anisotropic (strongest) alnico magnets.

Significant differences (see copper nano-rods) were found in the nano-scale morphologies, and especially in the structural/chemical makeup of matrix phases for different alnico magnet types. One key observation was that the best alnico, which contains one and a half times the Co content of the classical alloy, appears to “waste” nearly half of this Co by trapping it in the matrix phase that is supposed to be non-magnetic. Recent

results suggest that this useless Co may even degrade the magnetic strength. These findings direct us to substitute lower-cost elements—e.g., Ni, Cu, Mn—for the Co, if possible, saving up to 20% of the alloy cost and perhaps improving the magnets. Linked microstructure and magnetic domain observations showed that promise for raising alnico strength also lies at the 10–100 micron scale, prime for powder metallurgy methods. These pathways to improved alnico should allow to double the energy product and reduce the cost by at least 10%, in contrast to the predicted upward cost trajectory for Nd-Fe-B magnets.

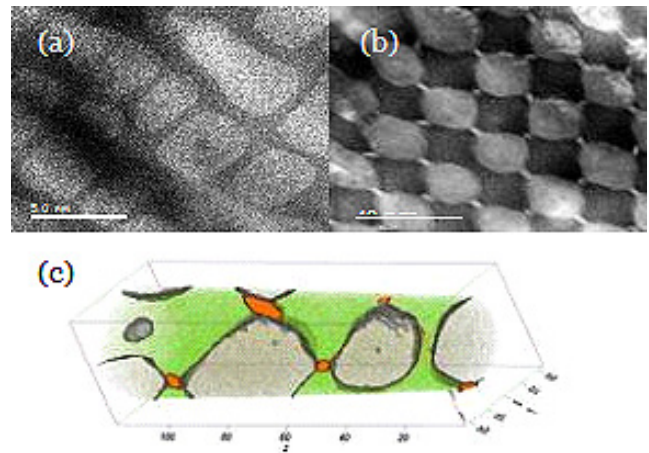


Figure 1. Figure showing (a) STEM image of the 5–7 alloy showing the ‘brick-and-mortar’ morphology, and (b) showing a ‘mosaic-tile’ morphology in alnico 8. Atom probe tomography (APT) (c) shows the isolated copper (orange) at the ‘tile’ points in 8. The Fe-Co phase is light gray regions. APT was obtained with collaboration of M. Miller at the ORNL ShaRE User Facility, sponsored by DOE’s Basic Energy Sciences (BES).

Electrochemical Energy Storage



High-Energy Lithium-Ion Batteries for EVs

Envia has developed lithium battery technology for EVs with very high energy density, thus significantly lowering the cost.

Envia Systems and U.S. Advanced Battery Consortium

Lithium-ion (Li-ion) batteries power most electrified vehicles on the market today. Battery pack costs approach 50% of the cost of the car; as a result, the EV market is unlikely to grow fast unless the battery pack costs are reduced dramatically. Battery costs can be dramatically reduced by using electrode materials that store more energy. Increased energy storage reduces the weight and the cost of the electrode materials. To achieve cost parity between EVs and gasoline-powered vehicles, batteries will require more than a 50% increase in the energy storage of today's state-of-the-art Li-ion batteries. Economies of scale cost reduction cannot account for such reduction because material costs are the majority of these electrode materials. Optimization of these electrode materials is the key to unlocking the EV market.

Envia has met a majority of the stringent USABC requirements for EV batteries while dramatically lowering costs. Gravimetric (214 Wh/kg) energy and power requirements, as well as the aggressive operating temperature environment targets, have been demonstrated at the cell level. In addition, cells with a similar cathode material paired with a silicon-carbon anode for an ARPA-E program have demonstrated nearly twice the gravimetric energy (400 Wh/kg) in early testing, so further progress is anticipated. Battery life is still being validated and cell cost continues to decrease. With respect to energy density, Envia has met USABC goals for EVs, and all power metrics are greater than four times the target metrics. In addition, Envia has demonstrated that it can operate its cells in a wide temperature window of -40°C to greater than 50°C, which also meets USABC requirements.

The confidence in meeting the cycle life target of 1000 cycles is high because the available data is showing 97% capacity retention after more than 500 cycles while meeting the other energy and power performance goals. The currently available cycling data have been obtained using Envia's constant current cycling protocol. USABC DST (Dynamic Stress Testing) cycling is ongoing and data will be available in the near future (Figure 1). Preliminary calendar life results at 30°C from the latest cells suggest promising calendar life results.

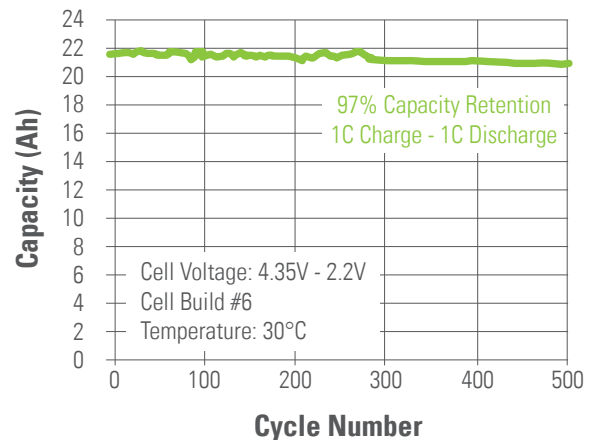


Figure 1. Cycle life of 22 Ah pouch cells from a recent cell build.

GenII Prismatic Cell Development

Building on new prismatic cell technology developed in the last USABC program, JCI initiated work to drive up volumetric energy density by 40% through material stabilization and novel cell design and processing.

Johnson Controls Inc. and U.S. Advanced Battery Consortium

In April 2012, Johnson Controls Inc. (JCI) began work to advance the new prismatic PHEV cell technology developed in the last USABC program to a GenII commercialization horizon. All tasks converge to reduce the Cost to Energy ratio from a baseline value of \$420/kWh to a stretch goal of \$250/kWh. In tandem, energy density will be advanced from the 275 Wh/L baseline to a 375 Wh/L target.

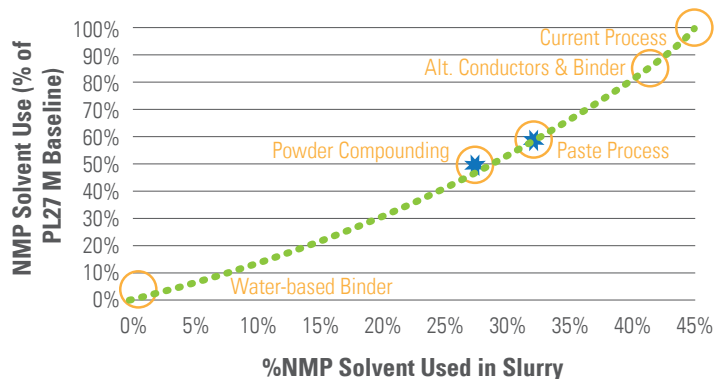
JCI's focus is on the domain of $\text{Li}[\text{Ni}_x\text{Mn}_y\text{Co}_z]\text{O}_2$ (NMC)/graphite chemistry, with specific aim at the higher nickel content variants in this family. These offer increased energy density, which translates to more capacity per cell and fewer total cells per system, thus delivering a lower system cost. JCI's strategy takes lower-risk materials beyond conventional limits through concerted material and processing innovation. While the materials of interest have already been optimized within the constraints of classic processing boundaries, the program pushes beyond these thresholds using novel slurry processing techniques to (1) reduce the quantity of the solvent N-Methyl Pyrrolidinone (NMP) used in cathode manufacturing (result: cost reduction), and (2) increase coated electrode energy density through relative increase in active material versus inactive constituents (result: increased Wh/L). Trials performed on two techniques of interest—dry compounding and paste mixing—both achieved targeted energy density increases (Figure 1), and samples are undergoing accelerated life tests.

High nickel material implementation requires improvement of critical market expectations, including life and abuse tolerance performance. Both performance areas require improved stability of electrodes and electrode/electrolyte interfaces. The baseline chemistry (not a high nickel stoichiometry) has shown remarkable thermal stability: under 20% capacity fade after 450 days at 70°C. This affords design margin for more aggressive use of the cells: higher nickel content, electrode

densification, increased upper voltage limit, and an expanded operating range.

'Out-of-the-box' mechanical design and assembly concepts are being investigated to reduce cost and minimize void volume of the cell. Prototypes have been made of novel can concepts, new current collector designs, fill-hole sealing strategies, and coatings applied to can interior and exterior for electrical insulation and cost reduction.

The goal is to deliver a 40% reduction in the central program metric: Cost to Energy ratio, broadly recognized as the gateway to widespread adoption of electrification technology.



Trial Results			
	Solvent Used	Slurry Density	Electrode Density
Baseline	Standard	Standard	Standard
Powder Compounding	-31.9%	+22.9%	+31.4%
Paste Mixing	-24.3%	+14.5%	+15.2%

Figure 1. NMP Solvent Use Continuum (mL/cell solvent used as a function of processing approach) and trial results (bottom).

EV Technology Assessment Program

New battery designs using lithium iron phosphate technology and many off-the-shelf parts approach the USABC EV and PHEV-20 goals.

K2 Energy and U.S. Advanced Battery Consortium

K2 Energy has successfully completed a Technology Assessment Program (TAP) wherein the USABC evaluated its lithium iron phosphate (LFP) technology against EV battery goals. The cells met many of the USABC goals for EV batteries and made progress toward the aggressive cost goal.

As part of the only LFP technology in the USABC portfolio, K2 provided two different battery configurations for testing (Figure 1). The first example (LFP165HES) was a commercially available 51Ah, 3.2V module, using commercial off-the-shelf components to save on cost. The second prototype (LFP45) was a 45Ah, 3.2V flexible prismatic pouch cell, using standard production electrodes and cell components.

The TAP included testing the available energy and power at multiple operating and storage temperatures, evaluation of the life of the battery in storage and in operation, and a technology cost assessment. All tests were conducted by both K2 and DOE's national laboratories using the USABC Electric Vehicle Battery Test Procedures Manual. Abuse testing was performed on each type of cell following the USABC Abuse Test Procedure Manual.

The test results indicate that this battery technology can provide the cycle life required for an EV battery,

while providing an energy density competitive with other battery technologies. The enhanced abuse tolerance of LFP was also demonstrated in both configurations.

The commercial technology cost assessment indicated that battery designs using this LFP technology can come close to achieving some of the aggressive cost targets set by USABC.

The results of this TAP also indicated that this LFP technology could potentially achieve most of the goals for a PHEV with 20 miles of EV range.



Figure 1. Example K2 Batteries under Test – LFP165HES module (left) and LFP45 cell (right).

A High, Specific-Energy PHEV Battery Pack with a Robust Thermal System

A 40-mile PHEV battery pack has been developed using a high-capacity cathode and a refrigerant-based, integrated cooling system.

LG Chem Power and U.S. Advanced Battery Consortium

One of the key roadblocks to the mass adoption of EVs is the development of a cost-effective, high-performance battery pack. To achieve this objective, LG Chem Power (LGCPI) has been working on a two-year program focused on developing a Lithium-ion (Li-ion) battery pack using the new class of high, specific-energy cathode materials that will meet USABC goals for a 40-mile PHEV battery pack. An important goal of the program is to develop an automotive-grade, self-contained battery pack using a refrigerant-based cooling system.

Using cells containing the manganese-rich cathode, laminated packaging, and the Safety Reinforcing Separator, LGCPI carried out development and optimization studies to meet USABC targets for performance, life, and cost. This cathode shows the highest capacity among all the cathode materials currently being studied (greater than 250 mAh/g). To obtain such high capacity, one needs to charge cells to voltages as high as 4.6V. This imposes a significant limitation on the use of electrolytes commonly employed in Li-ion cells. The material is also characterized by low power at low states of charge, which limits the usable energy and shows strong dependence of life on charge voltage (Figure 1, top). Use of electrolyte additives and/or surface treatments has been found to significantly improve the life of the cells (Figure 1, bottom).

LGCPI carried out a number of module and pack designs to improve the robustness, volumetric efficiency, and manufacturability using the refrigerant-to-fin cooling concept (Figure 2). The packs that were assembled with the optimized components have been subjected to drive cycles to assess the efficacy of this thermal management system. These packs will be delivered to DOE's national laboratories for testing.

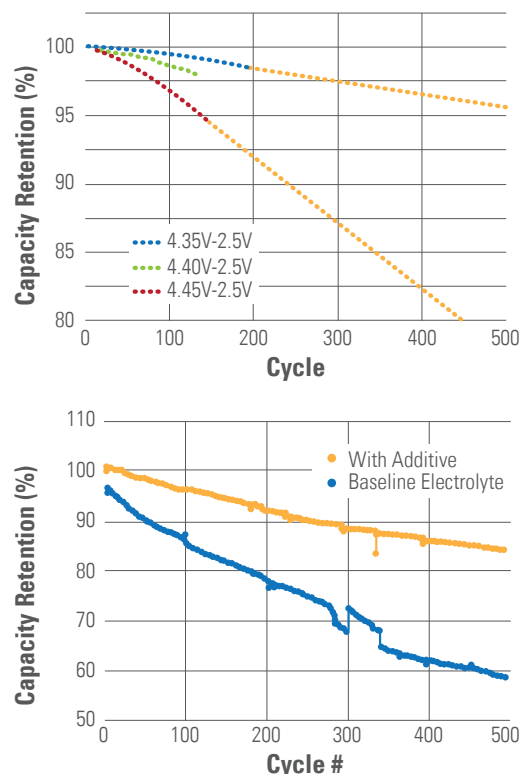


Figure 1. Top: An example of strong dependence of cycle life on charge voltage; Bottom: Usefulness of electrolyte additive to augment life.

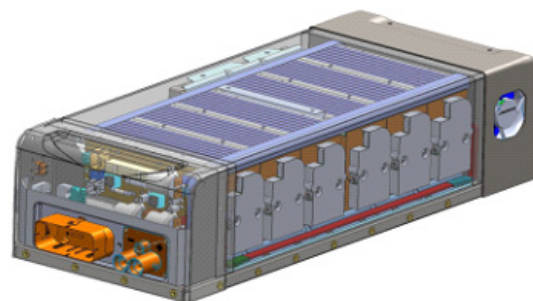


Figure 2. Schematic of the PHEV 40-mile pack. The thermal chamber (compressor, the cold plate, and the evaporator) is on the right, while the electrical chamber is on the left.

Scale-Up and Production of Low-Cost Nickel/Manganese/Cobalt Cathode Material

BASF has developed and scaled-up the production process for three nickel/manganese/cobalt cathode materials. Two such materials are currently in production in BASF's plant in Elyria, Ohio, and the final material will be produced in the production plant in the first quarter of 2013.

BASF

According to multiple cost models from DOE national laboratories and from battery developers, the cathode material dominates high-energy battery cost. The production of low-cost cathode materials depends on the proper selection of raw materials and a cost-effective production process. There are also many requirements for chemical purity, physical characteristics, and electrochemical performance that must be met.

This project aimed to scale-up and reduce the production cost of nickel/manganese/cobalt (NMC) cathode materials. As a result of this project, BASF has developed and scaled-up the production process for NCM 111, 523, and 424 (numbers represent the relative ratios of the three components). The first two materials are in production in BASF's plant in Elyria, Ohio, and the final material will be produced there in the first quarter of 2013. BASF has been able to qualify both NCM 111 and NCM 424 for use in EV and PHEV applications through independent testing by SKC PowerTech.

BASF has recently shifted much of the research and development work to the production of NCM 424. Results from the initial lab work have been used to identify the major production elements that are critical for the end product performance. Work with NCM 424 has progressed through the pilot plant stage and is in line for process transfer to production in early 2013. BASF has demonstrated that with its existing pilot plant equipment, it can produce NCM 424 consistently with minimal lot variation. Figure 1 shows 2C (5 ampere) charge discharge cycle life results from cells made with blends of BASF's NMC111 and LMO, where LMO is LiMn_2O_4 spinel, and another cell using a blend of NMC 424 and LMO. BASF will continue to focus on

precursor improvements and modifications in order to improve the quality of the NCM 424.

BASF has also worked on the production of the high-energy NCM (HE-NCM). Although there is still ongoing research to improve the material, BASF has made progress, improving its performance as well as understanding of the critical production parameters. BASF has produced enough HE-NCM to provide samples to customers and research partners during the past year.

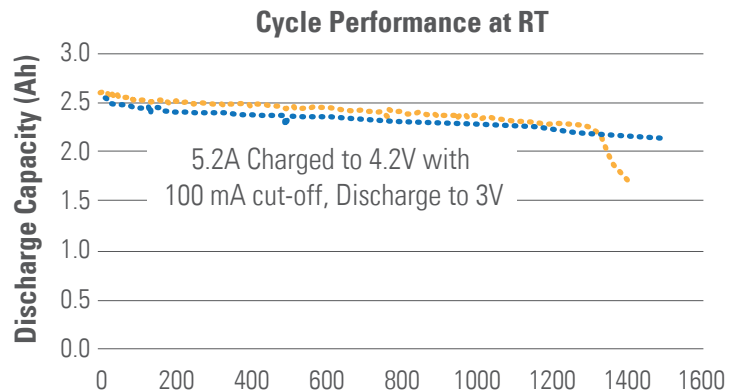


Figure 1. Cycle life data of NMC111/LMO blend and NMC424/LMO blend at room temperature (RT), appropriate for long-range PHEV and EV applications.

Modeling and Understanding Lithium-Ion Battery Performance and Cost

A free BatPaC model provides researchers, product developers, and policy makers with a tool for understanding Li-ion battery cost for transportation applications.

Argonne National Laboratory

The recent penetration of Lithium-ion (Li-ion) batteries into the vehicle market has prompted interest in projecting and understanding the costs of this family of chemistries being used to electrify the automotive powertrain. Additionally, research laboratories throughout the world are developing new materials for Li-ion batteries every day. The performance of the materials in the battery directly affects the energy density and cost of the full battery pack. The development of a publically available model that can project bench-scale results to real-world battery pack cost and performance would be of great use. The battery performance and cost (BatPaC) model represents the only public domain model that captures the interplay between design and cost of Li-ion batteries for transportation applications (available free-of-charge from www.cse.anl.gov/batpac). This model has been subject to many private and public peer reviews by experts in academia and industry.

The first version of BatPaC with supporting documentation (100+ page report) was distributed on November 1, 2011. Since this release date, more than 465 independent downloads have occurred worldwide. The majority of downloads originated within the United States. Industrial users, from high-profile start-ups to world leading large capital companies, make up the largest percentage of downloads.

The battery pack design and cost calculated in BatPaC represent projections of a 2020 production year and a specified level of annual battery production, 10,000–500,000. The bottom-up calculation approach accounts for every material and manufacturing process required. The calculated cost to the original equipment manufacturer (OEM) includes charges such as warranty, overhead, and pack integration components (battery management system, disconnects, etc.). An example of output from the model is shown in Figure 1. For high-energy batteries, power is relatively inexpensive. For the 30 kWh case, a battery of this chemistry has a minimum power level above 120 kW. For the low-energy case, the cost of additional power is significant. The smallest total energy content for the material in this study that can deliver 120 kW is approximately 7 kWh. BatPaC comes with six default Li-ion cell chemistries, but is designed so all material inputs may be changed by the user.

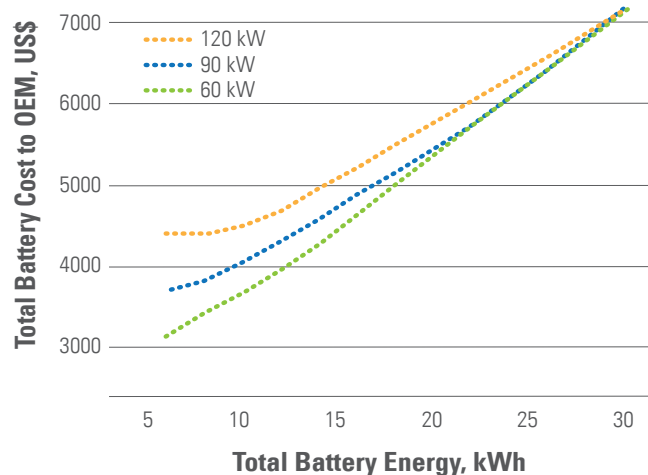


Figure 1. Total cost to OEM as a function of power and energy for a 360V NMC333-Gr battery at a production rate of 100,000 batteries per year.

Computer-Aided Analysis Methods for Lithium-Ion Battery Design Developed and Deployed

CD-adapco, Battery Design, Johnson Controls Inc., and A123 Systems are working on validated analysis methods for the spiral wound battery cell design to proliferate the use of computer-aided engineering in the design of Lithium-ion battery systems. An initial version of this code is now available to the public.

CD-adapco

The use of computer-aided analysis in the design of Lithium-ion cells is a growing field. Many experts in the field have developed extensive models for this physical problem. However, to achieve a general acceptance of such techniques, they need to be included in a widely accessible tool.

This project aims to introduce comprehensively validated numerical models into the widely accepted computer-aided engineering tool, STAR-CCM+. This objective should then lead to the proliferation of usage of such methods and ultimately allow designers to more effectively design Lithium-ion battery modules and packs. Of primary interest are the coupled thermal-electrochemical processes that dominate a cell's performance.

The project includes two Lithium-ion cell manufacturers and utilizes their products as platforms for validation work. Such validation work is ongoing and remains confidential. However, Figure 1 depicts screen shots of example cylindrical battery cells displayed within STAR-CCM+. These cells are undergoing pulse discharges, and both the voltage and maximum and minimum temperatures are plotted. The fundamental cell models have either a physical basis, using the original work of Newman et al. (1994), or use equivalent circuit models. These cell models capture the effect of the internal design of the cell, as well as the Lithium-ion chemistry used; all of which is contained in a single file that can be imported into STAR-CCM+. The user can then duplicate and connect the cells to produce a module or pack, which can then be combined with a cooling system or geometric details of the pack hardware to create a very high-resolution model. Figure 2 shows an example of a pack using pouch type cells instead of spiral wound cylindrical cells.

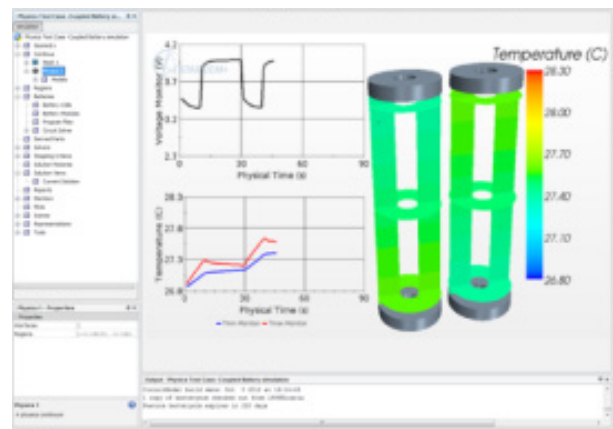


Figure 1. Screen shot of a two cell analysis within STAR-CCM+.

At this point in the project, a first release of this code has been made available to the public. This is supported through CD-adapco's customer-facing team.

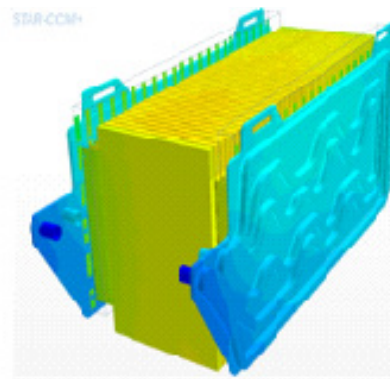


Figure 2. Example module using 42 cells, courtesy of Automotive Simulation Centre, Stuttgart, Germany.

Cell Fabrication Using Advanced Battery Materials

ANL's Cell Fabrication Facility has expanded the laboratory's capabilities so that promising next-generation battery materials can be tested and diagnosed from the lab bench-level to industrially relevant cell sizes.

Argonne National Laboratory

With the recent addition of new battery facilities, ANL has the ability to scale-up its most promising new battery materials discoveries and then manufacture working prototypes for detailed evaluation.

From basic battery materials research and process scale-up to fabrication and performance testing, ANL has expanded its capabilities so that nearly every aspect of battery research and development (R&D) can now be done onsite. The laboratory's new facilities allow ANL scientists to evaluate novel battery chemistries in a more practical and timely manner, helping to speed the validation to ultimate commercialization of advanced battery materials.

Of particular interest is a high-energy lithium-manganese-rich (LMR-NMO) cathode ($\text{Li}_{1.2}\text{Ni}_{0.3}\text{Mn}_{0.6}\text{O}_{2.1}$). With its exclusion of cobalt metal, the cathode should result in a lower material cost. This material offers a 30%–50% energy increase over current materials. It was originally made by R&D staff at ANL and, based on favorable results from the program's Materials Validation effort, was selected to be scaled-up into kilogram quantities at the laboratory's Materials Engineering Research Facility (MERF).

The MERF, using its production-ready processes for new electrode (and electrolyte) materials, was able to make a 10 kg batch of this LMR-NMO cathode. One kg was then delivered to the Cell Fabrication Facility (CFF) in early March 2012.

The CFF allows scientists to manufacture battery cells (both pouch and 18650 cells) and battery electrodes for research purposes. Outfitted with state-of-the-art pilot-scale production equipment, the climate-controlled facility is one of a few of its kind in this country. After optimizing the electrode mix, the CFF made high-quality single-sided and double-sided electrodes with this new

cathode. Several dozen pouch cells were then built in the CFF with these electrodes in a xx3450 cell format with approximately 400 mAh capacity, some of which are undergoing performance testing within ANL's Electrochemical and Diagnostics Laboratory. The initial performance of the cells was consistent with the results from the ANL screening activity and benchtop experiments.

The preliminary results show that this cathode can deliver an impressive capacity of 250 mAh/g. Observations made by Diagnostics and the Post Test Facility indicated areas for improvement, which provided valuable feedback to the researchers and MERF to make further optimizations to the cathode material.



Figure 1. ANL engineering assistant operates a state-of-the-art electrode coating system in the CFF to make the positive electrode used in prototype Lithium-ion cells.

AutoLion™: A Thermally Coupled Lithium-Ion Battery Model

A CAE tool for Li-ion cell and pack engineering has been released that allows for unparalleled simulation capabilities, enabled by a thermally coupled approach to battery modeling.

EC Power

EC Power has worked with its university and industrial partners to develop a first-of-its-kind, commercially available, computer-aided engineering (CAE) tool for large-format Lithium-ion (Li-ion) cell/pack development—AutoLion™.

Many of the obstacles currently facing EV engineers involve properly managing the expensive Li-ion battery pack in an EV that is highly sensitive to thermal conditions. Poor thermal management results in cell imbalance, poor battery performance, decreased cycle life, and potentially hazardous safety events such as fire or explosion.

EC Power's proprietary thermally coupled battery (TCB) modeling technology, AutoLion™ is able to capture the highly complex interaction between temperature and battery performance, while *simultaneously* calculating thermal and electrochemical outputs, leading to significant new simulation capabilities and technical innovations.

For example, Figures 1 and 2 illustrate a pack simulation where an original equipment manufacturer wanted to analyze the effects of thermal management on cell balancing for a 2.8 kWh battery pack, consisting of a serially connected string of 12 "cell groups;" each cell group contains two cells in parallel. The pack is initially at -10°C and undergoes a 1C discharge, along with heating by warm air pre-heated at 50°C. Figure 2 highlights a current imbalance, as a result of cell 1 remaining substantially colder than its parallel-connected partner, cell 2, during pack heat-up. This pack simulation of 1 hour discharge takes only 15 minutes on an 8-central processing unit workstation, dramatically reducing the time needed for product development.

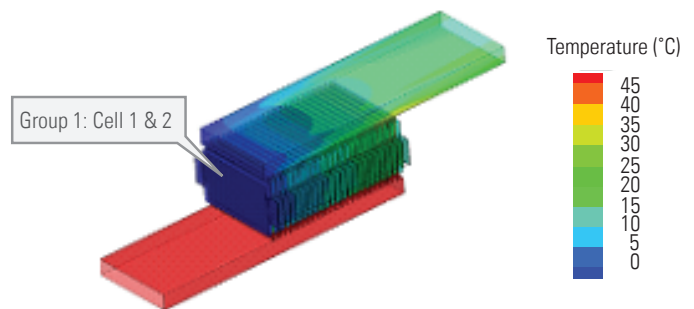


Figure 1. Thermal contours at t=500 seconds under cold-start discharge scenario.

AutoLion™ has been developed in the form of several tools aimed at simulating everything from the detailed 3D design of cells and packs to Li-ion battery systems. Each tool has been validated over a wide range of temperatures and discharge/charge rates. Further, each tool utilizes an advanced materials database that incorporates materials relevant to state-of-the-art Li-ion batteries, tested under extreme conditions encountered in automotive applications. Finally, battery pack safety has been extensively evaluated and new insight has been generated using these CAE tools.

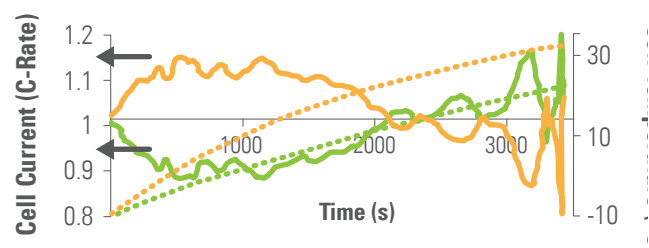


Figure 2. Current and temperature of cells #1 and #2 (group 1); cell 1: green, cell 2: orange.

Investigation and Improvement of High-Voltage Cathode Material

A team of researchers from multiple institutions used a variety of experimental and theoretical techniques to understand the impact of the atomistic character of a high-voltage cathode material on its performance.

Lawrence Berkeley National Laboratory

One of the promising cathode materials being investigated for use in long-range PHEVs and EVs is the high-voltage nickel/manganese spinel, $\text{LiNi}_{0.5}\text{Mn}_{1.5}\text{O}_4$, or LNMO. This 5V cathode material was chosen by the Exploratory Research Program to be a model material to study high-voltage electrolyte stability issues. Although this material has lower capacity than other advanced cathodes, its high voltage might allow the use of packs with fewer cells in series while still providing required power, thus lower total pack costs. Among several questions, issues associated with the relative amounts of Mn^{3+} and Mn^{4+} were investigated, as well as the impact of disorder on rate and cycle stability.

A collection of scientists from multiple institutions (Arizona State University, Army Research Laboratory, LBNL, Massachusetts Institute of Technology, PNNL, University of Rhode Island, University of Texas at Austin, and University of Utah) worked collaboratively on the material and associated high-voltage electrolytes. The group identified key performance parameters that allowed for the design and synthesis of a specifically designed material with high rate and excellent cycleability *versus* lithium. Through a combination of X-ray and neutron diffraction, nuclear magnetic resonance, Fourier transform infrared spectroscopy, X-ray absorption spectroscopy, single crystal performance and diagnostics studies, and first principles calculations, investigators determined that disorder of the Ni-Mn components resulted in improved rate capability and that high levels of Mn^{3+} played little role with regard to cycleability or rate. An example of these findings is provided in Figure 1, which shows the percentage of capacity obtained at 5C rate versus C/10 rate in a collection of materials

with different Mn^{3+} contents. This finding is important because it offers the opportunity of designing materials with low contents of this ion, which should improve life as Mn^{3+} is more prone to dissolution, while preserving maximized performance (durability and power). This result, combined with additional research on material morphology and doping, will be considered in the synthesis of a next-generation material with improved cycleability against graphite.

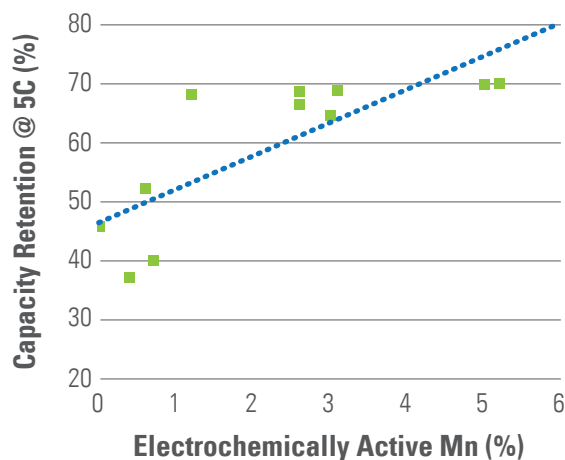


Figure 1. Ratio of specific capacity obtained during the first cycle at 5C versus C/10 rate against the Mn^{3+} content in LNMO samples made under different conditions.

A New Synthesis Approach to High-Energy Manganese Rich Cathodes

A new synthesis approach for the high-voltage, high-capacity, lithium-rich, manganese-rich cathode materials leads to significantly reduced voltage fade on high-voltage cycling.

Argonne National Laboratory

Li_2MnO_3 composite electrode structures, such as 'layered-layered' $x\text{Li}_2\text{MnO}_3 \cdot (1-x)\text{LiMO}_2$ ($M=\text{Mn, Ni, Co}$), are receiving attention because they provide rechargeable capacities up to 250 mAh/g between 4.6V and 2.0V. However, electrochemical 'activation' above approximately 4.4V alters the structure of these materials and sets in motion a gradual phase transformation that lowers the discharge voltage of the cells, thereby lowering their energy and power output. In an attempt to combat this voltage decay, a new synthesis technique to fabricate $x\text{Li}_2\text{MnO}_3 \cdot (1-x)\text{LiMO}_2$ electrode materials with greater resilience to internal phase transformations is being explored.

As can be seen in Figure 1, the performance of 0.5 $\text{Li}_2\text{MnO}_3 \cdot 0.5 \text{LiMn}_{0.5}\text{Ni}_{0.5}\text{O}_2$ cathode synthesized *via* a Li_2MnO_3 precursor shows high capacities of approximately 250 mAh/g at low rates ($\sim C/15$ or ~ 17 mA/g) and approximately 200 mAh/g at nominal rates ($\sim 1C$, or 250 mA/g). Remarkably, the voltage profiles quickly stabilize with respect to the initial 10 cycles. Figure 1 also shows charge and discharge curves to 35 cycles between 4.6V and 2.0V for a lithium half-cell at room temperature. This material displays good stability and capacity retention over extended cycling to high voltage. X-ray absorption fine structure (EXAFS) data (not shown) of fresh cathode materials compared to cathodes cycled up to 50 times (between 4.6V and 2.0V) reveal clues into the stability of the materials. Mn atoms are present in a predominantly Li_2MnO_3 -like environment, and significant changes to local structure occur during initial cycles. The local Ni environment is virtually unchanged after 50 cycles with respect to its original structure. Thus, the Li_2MnO_3 template may allow the formation of a unique ordering of Mn and Ni

conductive to the structural stability of local domains. It seems likely that the voltage fade is related to the activation process of the Li_2MnO_3 component and set in motion by the structural/ chemical changes that occur during that process.

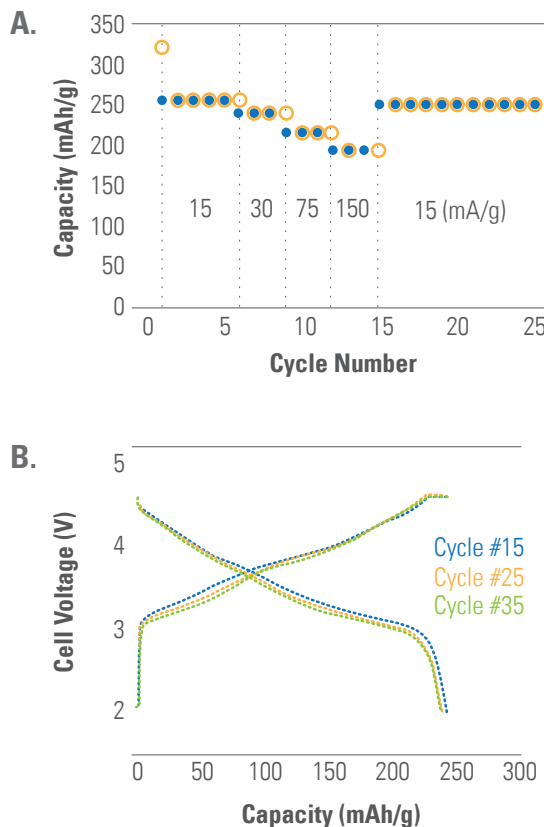


Figure 1. a) Rate data of a Li_2MnO_3 -based $0.5\text{Li}_2\text{MnO}_3 \cdot 0.5 \text{LiMn}_{0.5}\text{Ni}_{0.5}\text{O}_2$ cathode; (b) Voltage profiles of the cell in top figure up to 35 cycles (15 mA/g).

Lithium-Ion Electrolytes with Wide Operating Temperature Ranges

This project has discovered new electrolyte blends with significantly improved performance at low temperature that maintain life at high temperature—a critical need in PHEV and EV batteries.

Jet Propulsion Laboratory

As automakers produce and sell more vehicles with all electric range, the ability of advanced batteries to operate at low and high temperature becomes increasingly important. Poor high-temperature stability leads to shortened battery life, and poor low-temperature performance leads to reduced range for drivers. This project has identified a number of new electrolyte and salt blends that provide much improved low-temperature performance while maintaining good high-temperature life.

The electrolyte development work includes (1) optimization of carbonate solvent blends; (2) use of low-viscosity, low-melting ester-based co-solvents; (3) use of fluorinated esters and fluorinated carbonates as co-solvents; (4) use of novel “solid electrolyte interphase promoting” and thermal stabilizing additives; and (5) use of alternate, lithium-based salts.

This group has characterized a number of cells using the composition mesocarbon microbead carbon/LiNiCoAlO₂ using electrolytes with wide operating temperature range. One of the electrolyte formulations investigated, 1.20M LiPF₆ in EC+EMC+MP (20:20:60 vol %) (EC=ethylene carbonate, EMC=ethyl methyl carbonate, MP=methyl propionate), was demonstrated to have excellent low-temperature rate capability (Figure 1).

In an attempt to improve the life, especially at high temperature, formulations incorporating mono-fluoroethylene carbonate (FEC) were investigated. In particular, the electrolyte 1.20M LiPF₆ in EC+EMC+MP (20:20:60 vol %) + 4% FEC was evaluated at low and elevated temperature. Excellent performance was observed down to -50°C, with more than 75% of the room temperature capacity being delivered up to 2C rates with both formulations, and good cycle life was observed up to 40°C.

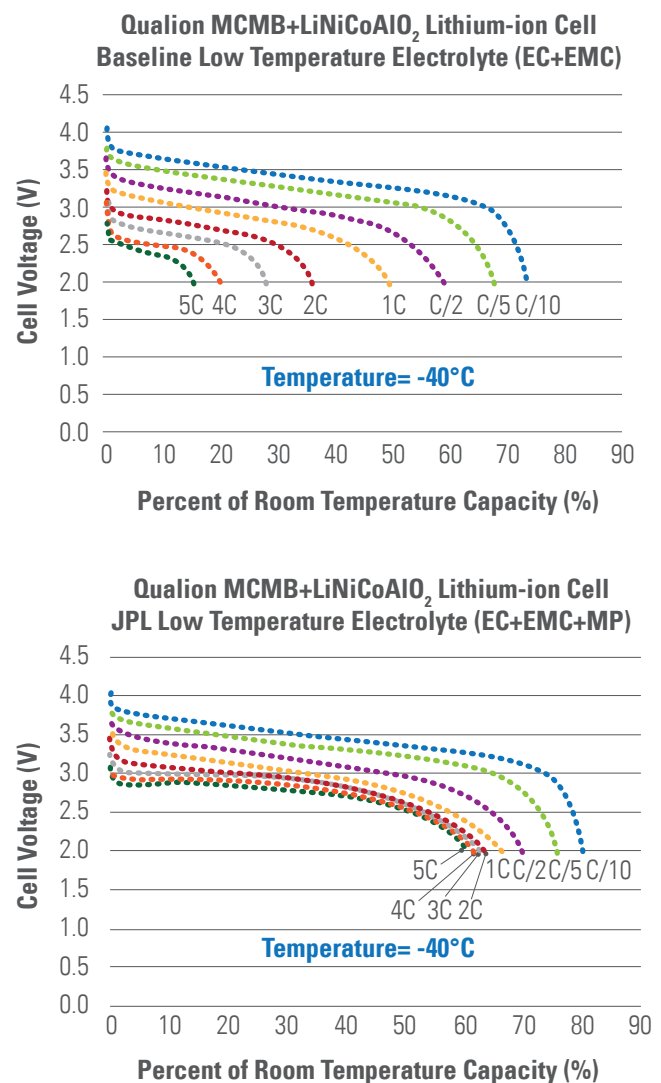


Figure 1. Discharge capacity for a baseline electrolyte (top) and an improved methyl propionate containing electrolyte (bottom) for cells cycled from C/10 to 5C.

Scale-Up of Promising Overcharge Shuttle for Industry Evaluation

Using its state-of-the-art labs and equipment, researchers can safely determine fast and economical ways of producing large quantities of advanced battery materials for commercial testing.

Argonne National Laboratory

The gap between small-scale laboratory research and high-volume manufacturing is one of the most significant hurdles in transitioning new battery materials to the market. Scale-up research and development (R&D) involves taking a laboratory-developed process and modifying it to enable economical, near commercial-scale production of a material.

When ANL scientists invented a redox shuttle additive—known as 2,5-di-tert-butyl-1,4-bis(2-methoxyethoxy) benzene or DBBB—to enhance the safety of Lithium-ion batteries during overcharge events, the amount they produced was sufficient for scientific testing. However, their process yielded too little material—less than 1 gram—for a company to perform validation and testing.

After only a few months of work at the Materials Engineering Research Facility, researchers scaled-up production of the molecule and sampled it to industry. Specifically, researchers took the formula and developed an improved, scalable process that created 1,576 grams in a single batch—enough to study and validate in a real battery cell.

In addition to providing sufficient material for commercial testing, another goal of process scale-up is to find economical ways to make a material. The bench-scale process used to discover DBBB would have cost 20 times more and generated 50 times as much waste as the scaled-up process. The new process also is three times faster.

The scale-up of a specialty material is not straightforward. Unlike the doubling or tripling of a cake recipe, it is not a matter of multiplying the amount of a chemical formulation by 1,000, 10,000, or more to make larger

quantities of a molecule. Other considerations—like time, temperature, concentration, mixing speeds, and even the chemical ingredients—arise when attempting to make vastly larger volumes for commercial testing and mass market production.

It is hoped that this new ability to scale-up material production will allow researchers to reduce the time between product innovation and commercial licensing and manufacturing. Not only will the payback to the taxpayer's investment in R&D be shortened, but innovation's contribution to the growth of the U.S. economy will be realized that much sooner.



Figure 1. Container of the DBBB overcharge shuttle additive scaled-up from 1 gram to kilogram quantities for commercial testing.

High-Capacity Hollow Silicon Nanofiber Anodes

A new approach to manage the issues of volume expansion and solid electrolyte interphase stability in Silicon anodes has resulted in successful cycling of a Silicon cell over 6,000 times at a capacity twice that of traditional carbon anodes.

Stanford University

Silicon (Si) offers almost 10 times the energy of today's best graphite anodes and is widely seen as a critical component of next-generation Lithium-ion batteries for PHEVs and EVs. Issues with Si anodes include large volume change upon cycling, as well as poor stability of the surface passivation film or the solid electrolyte interphase (SEI).

To overcome these issues, this project explores new types of Si nanostructures. Specifically, a variety of hollow and porous nanostructures have been fabricated, and their performance compared with other nanostructures. These hollow/porous nanostructures could act to minimize external volume expansion and produce stable SEI layers that will lead to more efficient long-term cycling.

Promising results were acquired from electrodes using a hollow Si nanofiber geometry. This structure is designed for SEI control: the surface region of the thin (*ca.* 40 nm) tube wall is oxidized, and this oxide layer acts as a constraint, promoting inward expansion of the Si material during lithiation (Figure 1, top). In this way, outward expansion of Si and repeated SEI fracture and electrolyte exposure is avoided. Thus, SEI formation is expected to be limited and less severe than in traditional geometries; this is demonstrated by the scanning electron microscopy (SEM) images in Figure 1, middle. The left image shows that a relatively extensive SEI film grows on tubes without the external oxide constraining layer after 200 cycles. The right image shows that a much more compact and uniform film grows on the tubes with the oxide layer after 2,000 cycles. This leads to better coulombic efficiency and lower overpotential in the cell. This geometry also leads to remarkable cycling behavior. Figure 1, bottom, shows the good capacity retention for 6,000 cycles at a rate of 5C.

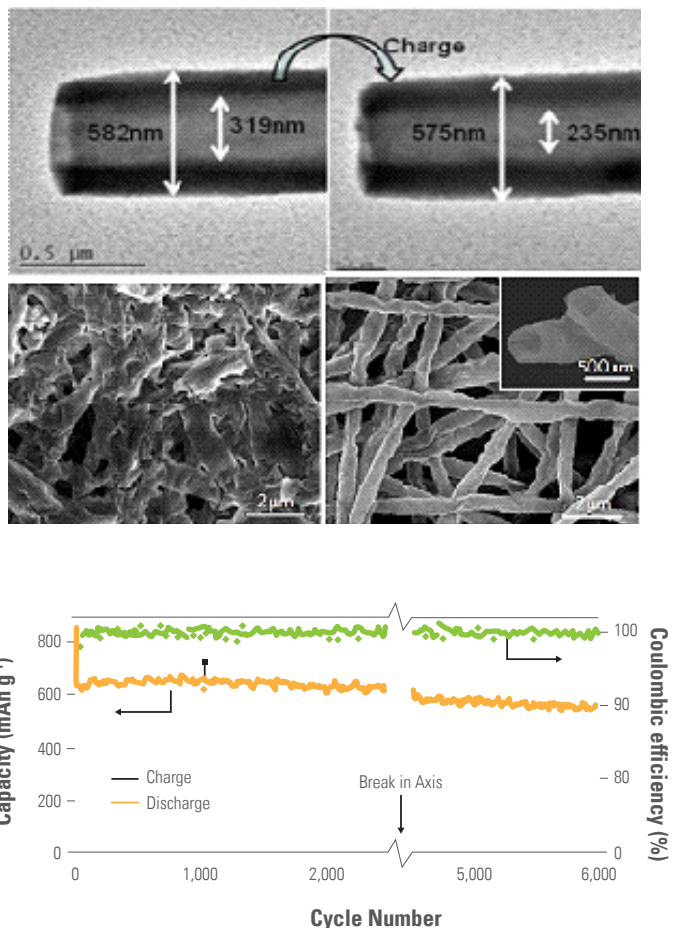


Figure 1. Top – SEM image of hollow Si nanotube showing closure of the inner diameter and stability of the outer diameter after lithiation; Middle (left) – continuous SEI growth of unconstrained nanotubes versus (right) stable SEI film after 200 cycles; Bottom – 6,000 cycles of Si cell using hollow nanotubes.

Single Crystal Diagnostics Leads to Improved Material Performance

Multiple diagnostics techniques show that spinel morphological design of high-voltage LNMO particles can impact its power performance by almost two orders of magnitude.

Lawrence Berkeley National Laboratory

One of the promising lithium-ion cathode materials being investigated is the high-voltage nickel/manganese spinel, $\text{LiNi}_{0.5}\text{Mn}_{1.5}\text{O}_4$ or LNMO. This 5V material offers the possibility of complete battery systems with many fewer cells and, as a result, reduced cost. The material was therefore chosen to be a model material to study high-voltage electrolyte stability issues. One of the studies focused on finding the optimum particle size and morphology for optimal transport while minimizing side reactions which, by default, is reduced by using large particles.

First, micron-sized LNMO single crystals in plate and octahedral shapes were synthesized. The main surface facets on the plates were determined to be (112) crystal planes, while the octahedrons were predominantly enclosed by the (111) crystal planes. Next, the transport properties of the crystal samples with different morphologies were compared using the Potentiostatic Intermittent Titration Technique (PITT) on composite electrodes using standard materials. The lithium chemical diffusion coefficient was calculated from the PITT results. Figure 1 compares the measured chemical diffusion coefficients during charge and discharge. Lithium diffusion exhibited concentration-dependent behavior in both crystal samples, which ranged from 1.9×10^{-16} to 1.2×10^{-14} cm^2/s in the plates and 2.4×10^{-14} to 1.6×10^{-11} cm^2/s in the octahedrons. Thus, diffusion in the octahedrons with (111) facets is at least two orders of magnitude higher than that in the plates with the (112) facets. The results demonstrate the importance of spinel particle-morphology design to lithium transport.

The incremental capacities and chemical diffusion coefficients were obtained during the charge and discharge of both crystal types. Two diffusion minima were observed on charge and discharge, and both correlated well with capacity maxima. The study suggests that lithium transport in the Ni/Mn spinel is likely limited by the movement of phase boundaries.

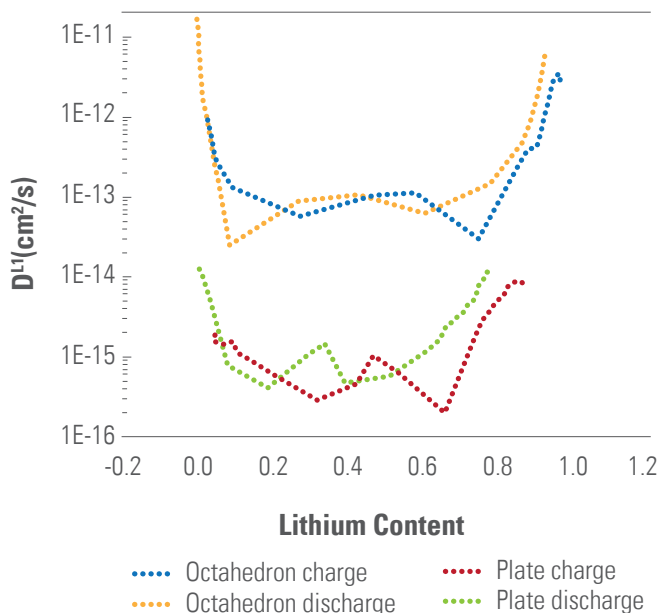


Figure 1. Chemical diffusivity comparison between the plate and octahedral shaped $\text{LiMn}_{1.5}\text{Ni}_{0.5}$ single crystals.

Technologies for Improved Safety of Lithium-Ion Batteries

TIAX LLC has developed methods to induce Li-ion cell internal shorts and thermal runaway during otherwise normal operation; TIAX is using these methods to develop technologies to improve the safety of Li-ion.

TIAX LLC

Concerns regarding the safety of Lithium-ion (Li-ion) batteries in EDV applications have been heightened by highly publicized safety incidents and ensuing recalls of Li-ion batteries used in portable electronics. In these failures, Li-ion batteries operating under otherwise normal conditions experienced an internal short (induced by foreign metal particles) that resulted in spontaneous thermal runaway with violent flaming and high temperatures. Such failures could be more devastating in EDVs that employ larger cells and packs. An important lesson from consumer Li-ion batteries is that improved manufacturing alone will not eliminate safety incidents—the safety-related failure rate of consumer cells is less than 1 failure in 10 million cells (i.e., better than six-sigma quality). Additionally, conventional safety technologies have been ineffective in preventing these incidents. There is therefore an urgent need to develop new technologies to prevent/manage such safety failures. The rarity of internal short-induced failures requires that such failures first be reproduced in the laboratory for refining and validating new safety technologies.

Informed by fundamental mechanistic studies, TIAX LLC developed methods to deliberately induce internal shorts in Li-ion cells. TIAX has successfully induced internal shorts in more than 100 commercial Li-ion cells by implanting metal particles, which in many cases led to thermal runaway (Figure 1) during normal operation. As can be seen in Figure 1, the cell temperature exceeded 800°C. TIAX also induced internal shorts in 18,650 Li-ion cells custom-built using its cell prototyping facility.

The information from such tests is allowing TIAX to develop key safety technologies. For example, experimental data were used to validate a Finite Element Analysis (FEA) model of thermal runaway in Li-ion cells, and the validated model is being used to develop cell and pack designs that can limit damage from thermal runaway (Figure 2). In addition, cell technologies are being developed to delay or suppress the growth of internal shorts. TIAX previously developed a technology to detect internal shorts before they become a threat to battery safety. TIAX is now maturing these technologies for implementation in EDV cells and packs.

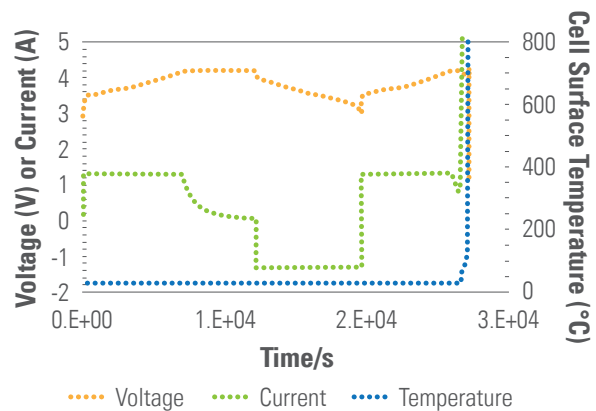


Figure 1. A123 Systems Gen PHEV cell calendar life results and projections at various temperatures, and 80% SOC.

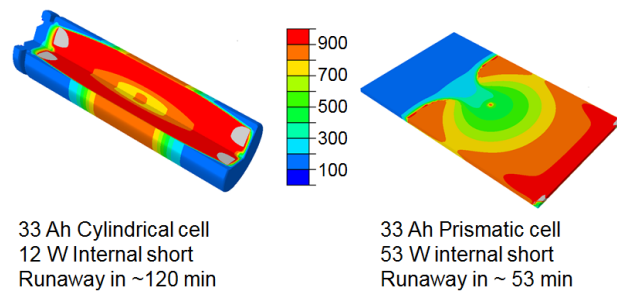


Figure 2. Simulations results (from a validated FEA model) showing the effect of the cell format on thermal runaway of PHEV cells following an internal short. The higher surface to volume ratio of the prismatic cell means that this cell tolerates internal short up to 4x higher power before thermal runaway occurs. The model allows visualization of the evolution of the cell temperature during thermal runaway.

In January 2013, TIAX introduced its Lithium-ion battery safety sensor system for detecting and pre-empting short circuits inside a Lithium-ion cell.

Use of Atomic Layer Deposition Coatings to Stabilize High-Voltage, High-Energy Cathode Materials

This project is evaluating coated, high-voltage, high-energy cathode materials to understand the ability of surface coatings to stabilize the materials' structures during high-voltage operation.

Brookhaven National Laboratory

Current Lithium-ion batteries are too expensive, weigh too much, and are too large for many high-energy automotive applications. Thus, researchers have been searching for higher-energy anode and cathode materials, like silicon and the lithium-rich/manganese-rich cathode materials, respectively. The latter show high capacity up to 280 mAh/g (at 4.8V) versus 170 mAh/g for today's state-of-the-art cathode materials.

However, these new materials suffer from a number of issues, including voltage fade during high-voltage cycling; high impedance; and metal dissolution, which leads to pore clogging and poisoning of the anode. One technique being pursued by multiple groups is to coat the cathode with a surface layer to stabilize the cathode/electrolyte interface.

This group has used time-resolved X-ray diffraction (TR-XRD) to quantify the structural changes in non-coated and atomic layer deposition (ALD)-coated (with Al_2O_3) lithium-rich/manganese-rich cathode material ($\text{Li}_{1.2}\text{Ni}_{0.17}\text{Co}_{0.07}\text{Mn}_{0.56}\text{O}_2$) during heating. As shown in Figure 1 (bottom), in the fully charged state (4.6V), when heated from room temperature to 600°C, the uncoated sample went through a phase transition from layered phase (R-3m) to the spinel phase (Fm3m) starting at approximately 350°C, which is believed to be associated with the observed voltage fade. In contrast, the starting temperature for this phase transition from layered to spinel for the fully charged ALD-coated sample was in the 450°C range, a more than 100°C increase (Figure 1, top). These results demonstrate the improvement in thermal stability obtained by the ALD coating of Al_2O_3 on $\text{Li}_{1.2}\text{Ni}_{0.17}\text{Co}_{0.07}\text{Mn}_{0.56}\text{O}_2$ materials.

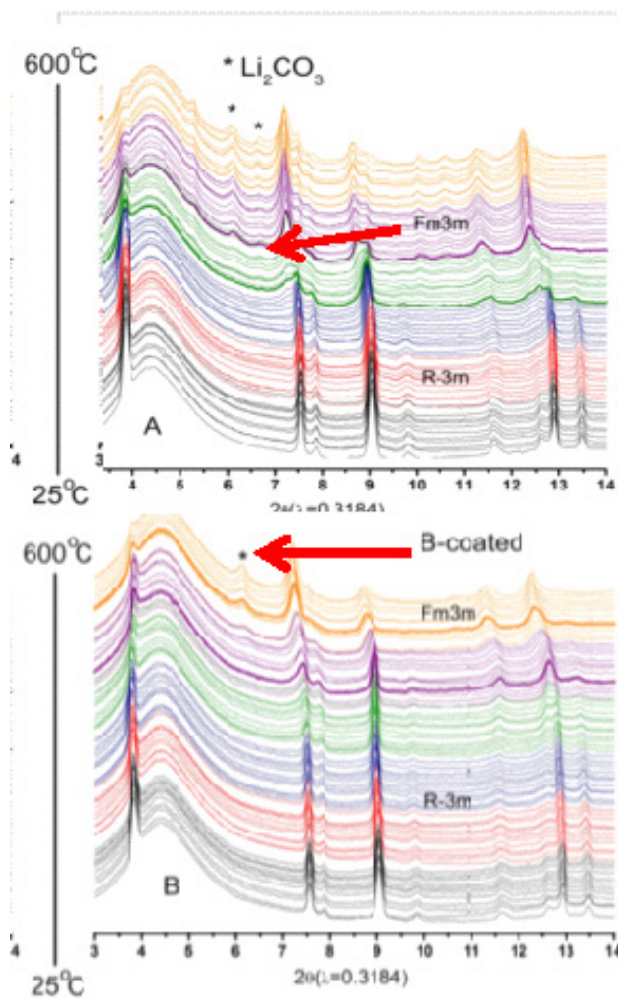


Figure 1. Crystal structure changes of fully charged cathode material $\text{Li}_{1.2}\text{Ni}_{0.17}\text{Co}_{0.07}\text{Mn}_{0.56}\text{O}_2$ with (bottom) and without (top) Al_2O_3 ALD coating studied by TR-XRD during heating from 25°C to 600°C.

Fuel Cells



Model Validates Performance and Cost Projections

Fuel cell stack model with 3M nanostructured thin-film electrocatalyst-based membrane electrode assemblies is validated with DOE-funded project data.

Argonne National Laboratory

A validated fuel cell model is needed to gauge the progress in research and development activities and to identify opportunities for further improvement in performance and cost. ANL developed and validated such a model for automotive systems using data from DOE-funded projects, and is using the model to supply information for the annual manufacturing cost updates by Strategic Analysis, Inc. (SA).

In the past year, ANL validated its model for a stack with 3M's nanostructured thin-film (NSTF) electrocatalyst-based membrane electrode assemblies (MEAs). As shown in Figure 1, the optimum system cost occurred at 0.15 mg/cm²; lowering Pt loading to 0.1 mg/cm² increased (rather than decreased) the system cost. ANL's performance model and SA's cost model both use NSTF MEAs in their 2012 reference fuel cell systems. ANL worked extensively with 3M to develop test plans for characterizing the performance of 50-cm² cells with NSTF MEAs for different Pt loadings in the ternary PtCoMn cathode catalyst over a range of operating pressures, temperatures, relative humidities, and fuel and oxidant stoichiometries. ANL used the data to validate and refine its models for the oxygen reduction reaction on the NSTF cathode, hydrogen oxidation reaction on the NSTF anode, and mass transfer in the NSTF anode and cathode catalyst layers.

ANL used the validated stack model to conduct single- and multi-variable optimization studies, and to determine the "best" conditions that lead to the lowest Pt content (in terms of g-Pt/kW) and system cost (\$/kW). Figure 1 summarizes the results from a representative study on the effect of Pt loading in the cathode catalyst on system performance and cost. These results show that for a system with a specified efficiency of 47.5% at rated power, the Pt content decreases monotonically with decreasing Pt loading, but the overall system cost is the lowest at an intermediate Pt loading of 0.15 mg Pt/cm² in the cathode. Another study showed that the Pt content and the system cost are lower for a system with a compressor-expander module that delivers compressed air to the polymer electrolyte fuel cell stack at 2.5 atm at rated power than for a system with a compressor that delivers air at a lower pressure (1.5

atm). Also, heat rejection is easier in the first system, as it allows operation at higher temperatures (lower $Q/\Delta T$) under demanding driving conditions and ambient temperatures.

Partnering with SA, ANL's analysis showed that under optimum operating conditions, the projected Pt content and system cost with current technology vary from 0.21 g/kW and \$46.1/kW for 47.5% system efficiency to 0.23 g/kW and \$48/kW for 50% system efficiency at rated power. Further performance improvement and cost reduction are needed, however, for stack and balance-of-plant components to meet the ultimate cost target of \$30/kW.

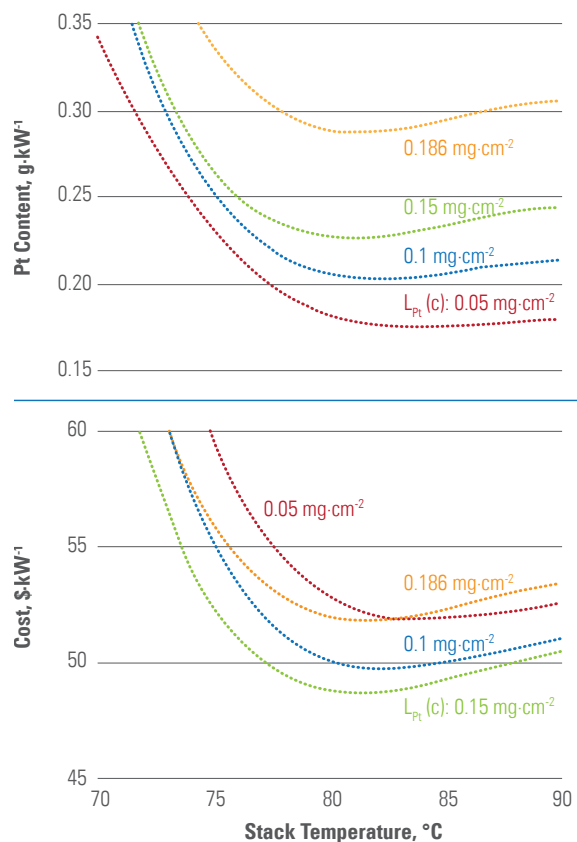


Figure 1. Effect of Pt loading in the cathode catalyst on Pt content and cost for system with 47.5% efficiency at rated power and fixed 0.05 mg/cm² Pt loading in the anode catalyst.

Model Prediction of Performance for Low Platinum Use

Reducing the amount of expensive platinum in fuel cells is necessary for lowering cost. However, predicting performance of low platinum fuel cells has been difficult. Using catalyst layer properties, a new model shows that an accurate prediction can be made.

Ballard

Cost and durability are the most important barriers to the commercialization of automotive fuel cell technology. Two of the most effective means for lowering the cost of a fuel cell system are lowering the size of the stack and lowering the loading of platinum. The size of a fuel cell stack is inversely related to the expected power density that can be achieved—the higher the power density, the smaller the stack can be. Fuel cell developers must be able to accurately predict power density when designing stacks. However, as many fuel cell developers attempt to lower platinum loading, the ability to accurately predict power density is diminished.

Ballard has developed a model that can accurately predict fuel cell performance at low platinum loading. As shown in Figure 1, at a loading of 0.05 mg of platinum per cm^2 of active area in the stack, the model prediction is capable of very closely estimating experimental performance.

The catalyst layer that enables the electrochemical reduction of oxygen is comprised of three phases: 1) electrically conductive platinum anchored on a high surface area support, 2) ion-conducting polymer, also known as ionomer, and 3) pores that allow transport of oxygen. The unique approach used in this project has led to the success of the model—instead of presuming the catalyst layer to be similar for all possible loadings of platinum, the input into the model takes into account the effect of loading on the porosity of the catalyst layer, as well as the content of ionomer in the catalyst layer. Furthermore, the model carefully accounts for the presence of product water in the catalyst layer. While one of the advantages of fuel cells is that only water is produced as a byproduct, the water that formed within

the catalyst layer can block oxygen from accessing the platinum catalyst, particularly when there is less platinum. The Ballard team modeled the level of water saturation throughout the catalyst layer from the adjacent membrane on one side, to the gas diffusion media on the other. Ballard studied water saturation as a function of platinum loading as the company had done with porosity and ionomer content, and the model inputs were adjusted accordingly.

As changes in the catalyst layer with material degradation are better understood, this model will be able to assist in predicting lifetime.

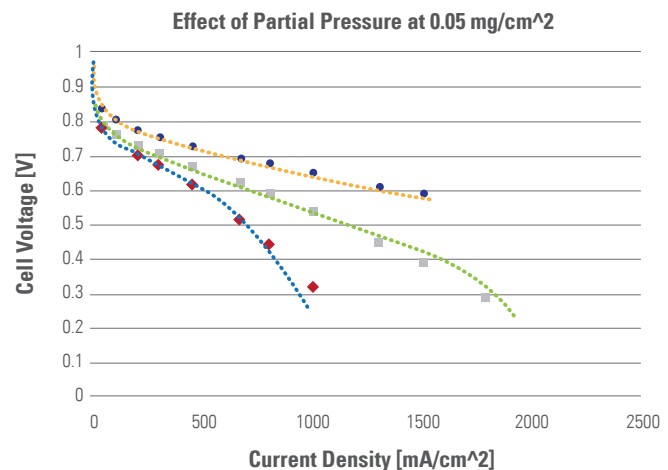


Figure 1. Experimental performance (points) versus model prediction (lines) at low platinum loading (0.05 mg platinum/ cm^2). The three experimental and simulated polarization curves are for the same BOT MEA at 100% RH, 5 psig, and 75 C for both anode and cathode, H_2 at the anode, and varying O_2 content with the remainder of the gas N_2 at the cathode.

Designing Durable Fuel Cell Catalysts

Fuel cell catalyst durability can be improved by tailoring catalyst properties and controlling system operating conditions.

Argonne National Laboratory

One primary challenge facing commercialization of automotive fuel cell technology is the durability of fuel cell materials, especially platinum-based (Pt) cathode catalysts. ANL has defined the primary reasons for the lifetime limitations of catalysts, and defined catalyst properties and operating conditions that potentially enable fuel cells to achieve the lifetime targets for automotive applications. This discovery will guide the development of catalysts that can simultaneously meet the activity, cost, and durability targets.

A fuel cell catalyst typically consists of small particles of Pt or Pt alloys on a high surface area support. By systematically varying the catalyst type and properties, utilizing cell degradation testing, and in-cell and out-of-cell advanced characterization techniques, the ANL-led team determined that the primary mechanism of catalyst degradation under load cycling is loss of catalyst surface area through dissolution of small particles and re-deposition to form larger particles. The team also determined that the size of the catalyst particle is the primary catalyst property governing catalyst lifetime as dissolution rates are highly dependent on particle size. Figure 1 shows the fraction of initial catalytic activity remaining after application of the U.S. DRIVE catalyst accelerated stress test for a variety of Pt and Pt alloy catalysts with various particle sizes. These results show that catalysts with particle sizes >5 nm have the potential to meet the catalyst durability target of <40% loss of initial activity.

The Team also determined the impact of various critical fuel cell operating conditions on the catalyst lifetime. As shown in Figure 2, catalyst lifetime can be extended by limiting the cell voltage, decreasing the rate at which the voltage of the cell is varied, lowering the amount of water in the catalyst layer, and reducing the operating temperature of the cell.

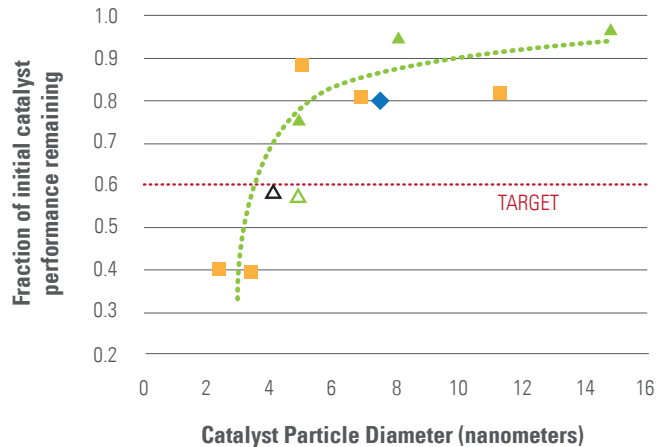


Figure 1. Fraction of initial cell performance remaining after durability testing as a function of initial mean diameter of the catalysts particles. Squares: Pt, Triangles: Pt₃Co, Hollow Triangles: Acid-leached Pt₃Co, Hollow black triangle: Acid-leached PtCo, Diamond: Pt₃Sc.

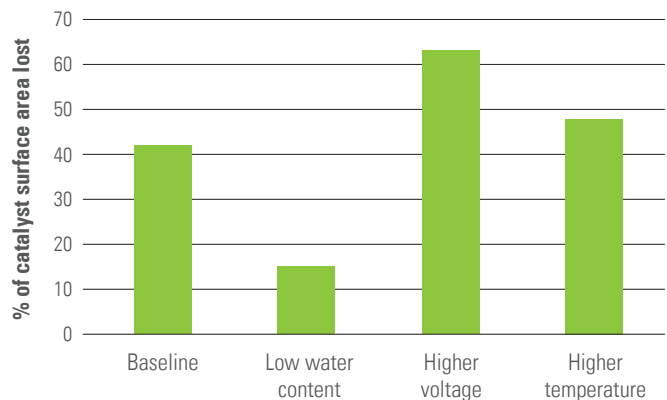


Figure 2. Percent of active catalyst surface area lost with load cycling under various fuel cell operating conditions.

Investigation of Micro- and Macro-Scale Transport Processes for Improved Fuel Cell Performance

Understanding of fuel cell fundamentals is improved by connecting characterization techniques to performance models and by making available the entire dataset to the fuel cell community.

General Motors

The ultimate capability of fuel cells is governed by transport processes. The maximum power density, and thus the size of the stack, is dependent on oxygen transport to the electrode surface. The transport of product water through the gas diffusion layer, and the back diffusion through the membrane into the anode catalyst, play a critical role in determining the performance of the fuel cell. Descriptions of the physics involved with these processes are required to develop optimal materials and designs to enable wide-scale automotive fuel cell commercialization.

As such, this collaboration has advanced the understanding through a multi-pronged approach that characterizes the relevant material properties utilizing existing and novel diagnostics; develops a multi-dimensional cell model for both single phase (gas) and two-phase (gas and liquid water); and generates a complete set of validation data from down-the-channel, or “macro-scale,” experiments. The complete data set has been made publicly accessible (www.pemfcd.org), a level of open disclosure described as “unprecedented” by one peer reviewer.

Key accomplishments in the recent past include understanding the impact of the device resistance for measuring water transport across the membrane and using the method to establish a good baseline correction for overall water transport across the membrane. The improvement in measuring water transport across the membrane has led to a significant improvement in the ability to predict water balance across the anode and cathode over a wide range of operating conditions.

Figure 1 below shows the measured and predicted cell voltage, along with the fraction of product water measured in the cathode exhaust. The model predictions were made using the dry model (red line) and the preliminary wet model (blue line). The predictions from the wet model closely match the observed experimental data and confirm the higher rate of water transport across the membrane during wet conditions. The wet model development is ongoing—further improvements to water balance calculations based on the prediction of phase change location in the diffusion layers are being added in the next phase of the project.

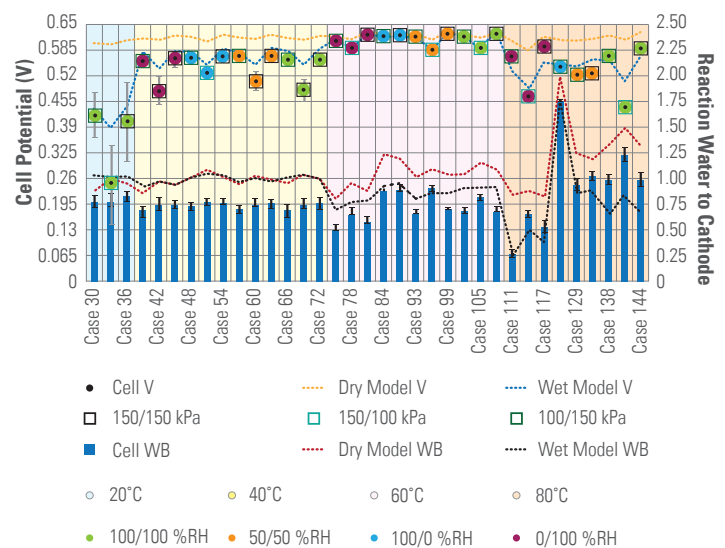


Figure 1. Cell voltage and fraction of product water in the cathode exhaust for various test cases.

Novel Non-Platinum Group Metal Electrocatalysts for Fuel Cell Applications Synthesized

Membrane Electrode Assemblies (MEA) prepared with new electrocatalysts show progress toward meeting durability, performance, and MEA cost targets without expensive platinum group metals.

Northeastern University

Fuel cell systems are projected to meet most of the requirements in terms of power density, fuel efficiency, and freeze capability. A major impediment to commercialization is the system cost. For example, platinum cost is the largest portion of the fuel cell stack cost, and therefore a reduction of the use of platinum (Pt) in fuel cells is necessary.

The collaborative project led by Northeastern University (NEU) uses a comprehensive material development strategy to eliminate Pt and other expensive Pt group metals. They employ novel new reaction centers for oxygen reduction, controlling metal support interactions and ensuring stability of the reaction center's electronic structure. The 2017 targets for non-platinum group metal catalysts include initial activity greater than 300 A/cm^2 of the electrode and less than 40% loss in initial activity after durability testing, contributing to MEA cost of less than \$3/kW.

Key project accomplishments include the development of new catalysts using metal organic frameworks, open framework structures, and non-metal polymer complexes. Figure 1 shows performance plots with catalysts derived from several precursors, with melamine showing the highest initial activity and intrinsic volumetric activity greater than 150 A/cm^3 . This catalyst, displayed in Figure 2, showed improved durability. The catalyst was subjected to Nissan's durability cycling protocol (square wave, 3 sec at 0.6 and 3 sec at 1.0V) for 1,600 cycles, then subjected to a carbon corrosion cycling protocol (1.0 to 1.5 V load cycling). No degradation in performance was observed during the catalyst cycling protocol, and although performance did degrade during the carbon corrosion cycling, much of this was found to be recoverable under constant load at 0.4 A/cm^2 . Recovery was possible up to 1,600 cycles, after which irreversible losses were observed.

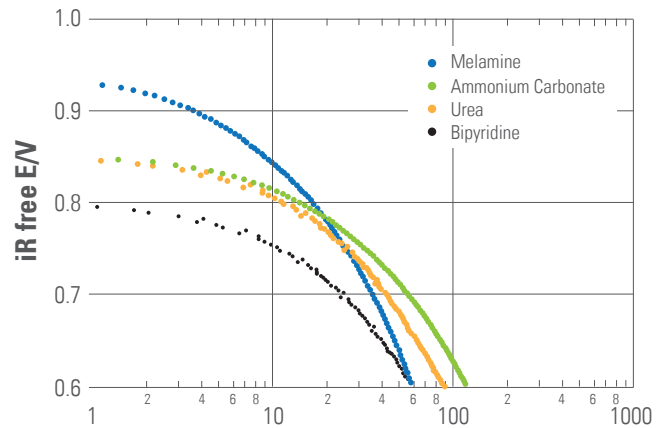


Figure 1. Performance plots for catalyst with various precursors showing an intrinsic activity for the melamine-derived catalyst of 176 A/cm^2 (obtained by extrapolation to 0.8 V).

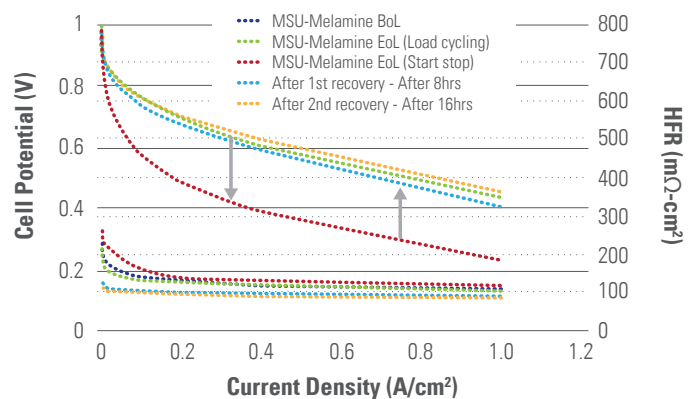


Figure 2. Performance of the melamine-derived catalyst before and after load cycling (0.6-1.0V), start/stop cycling (1.0-1.5V), and recovery (0.4 A/cm^2 constant load).

Materials



Optimization of High-Volume Warm Forming For Lightweight Sheet Alloys

Demonstrated the formability of an aluminum door inner design that achieved a weight savings of approximately 5 pounds over the steel original (approximately 13 pounds) using an unconventional non-isothermal elevated temperature forming method.

United States Automotive Materials Partnership

Traditional warm forming of aluminum refers to sheet forming in the temperature range of 200°C to 350°C using heated, matched die sets similar to conventional stamping. Non-isothermal warm forming (as used in this project) refers to a prescribed temperature difference between the die and the sheet, which has also been known to show enhanced formability characteristics within aluminum sheet. Phase 1 of this project determined the optimized non-isothermal warm forming parameters, while Phase 2 focused on the development and construction of a full-scale door inner panel. The extensive upfront thermal and formability studies guided the design of the die face and shape of the blank.

Following the construction of the die, manual and automated forming trials were conducted at two Tier 1 facilities. The manual trial verified concept feasibility and identified areas of the die that required modifications prior to the automated trial. The automated trial was used to demonstrate process repeatability, cycle time, and the formability window, while the forming cell included demonstrations of preheating, automation, and formability. Successful parts, as shown in Figure 1b, were formed with a sheet temperature in the window of 250°C +/- 10°C, with a room temperature die face using material from two material suppliers in both in-line and transverse to the rolling direction. Post-formability analysis demonstrated the dimensional accuracy of the process and commonality of alloy formability with respect to thinning and increased tensile yield; the latter is shown in Figure 2.

This work demonstrated that the optimized warm forming process provides sufficient formability in a production environment consistent with conventional stamping. The demonstration part realized a weight savings in aluminum of approximately 40% compared to steel. In addition, the part can be produced in a single draw without a re-strike operation. For these

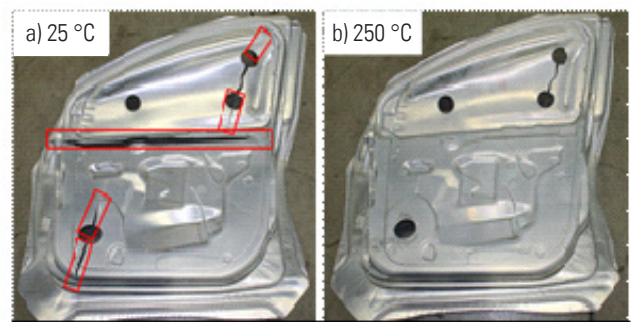


Figure 1. Door inner panel formed at 25°C shows splitting; at 250°C, the part forms successfully.

reasons, there is a high probability that the optimized warm forming process would be adopted by original equipment manufacturers and suppliers for the forming of various aluminum components in future efforts toward achieving mass savings.

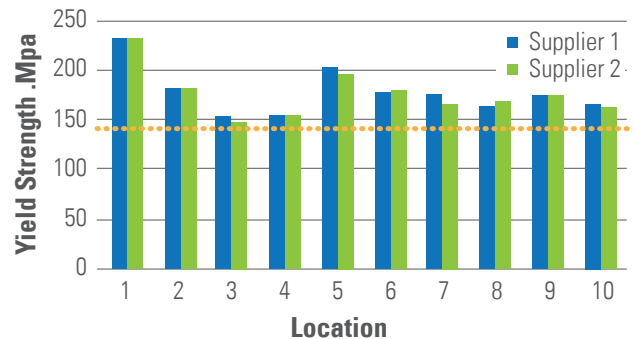


Figure 2. Yield stress behavior comparison of the post-formed door inner panels from Supplier 1 and Supplier 2 material; the dashed line indicates as-received yield strength (~139 MPa).

Integrated Computational Materials Engineering of Magnesium

Advancing the “community of practice” for integration of fundamental materials science knowledge of magnesium alloys into practical manufacturing outcomes.

United States Automotive Materials Partnership

USAMP has pursued “Integrated Computational Materials Engineering (ICME) of Magnesium” for several years as a project adjunct to a broader, comprehensive and international effort aimed at substantial weight reduction of light vehicle front-end substructures through incorporation of magnesium alloys. ICME has generally been identified with extensive use of computational methods over a range of length scales to enable prediction of material properties at the engineering scale. The approach has received recognition as a critical discipline when advanced as the “Materials Genome Initiative” by President Obama in 2011. The USAMP project has targeted magnesium alloys, in particular, as a focal point for ICME methodologies and, moreover, the all-magnesium substructures of “Magnesium Front-End Research and Development” as the physical objective of the efforts. Among other ongoing achievements, the project engendered a special symposium on Magnesium ICME, held at the 2010 Annual Meeting of TMS—The Minerals, Metals and Materials Society—in Seattle, Washington, and publication of more than a dozen peer reviewed papers in the field.

Figure 1 illustrates one recent outcome of the project wherein size distribution of precipitates of the Mg₁₇Al₁₂ (beta) phase in an AZ91D shock tower die casting produced by the super vacuum die casting process is quite accurately predicted from computer simulation of cooling rates (illustrated in the colored representation of the casting) using phase-field simulation and measured by transmission electron microscopy (TEM). Precipitation of second phases, such as the beta-phase in magnesium-aluminum alloys,

is a key strengthening mechanism, and this capability permits the materials scientist to predict a degree of this strengthening based on cooling rates, which are derived from computer software designed for such calculation for die castings. This type of simulation is among the first steps in determining the localized strength distribution in a complex casting based on a metallurgical process occurring on a microscopic scale, thereby linking two critical computational formalisms into a macroscopic prediction tool. Such a tool is anticipated to be an enabler for vehicle lightweighting through design optimization based on material performance prediction.

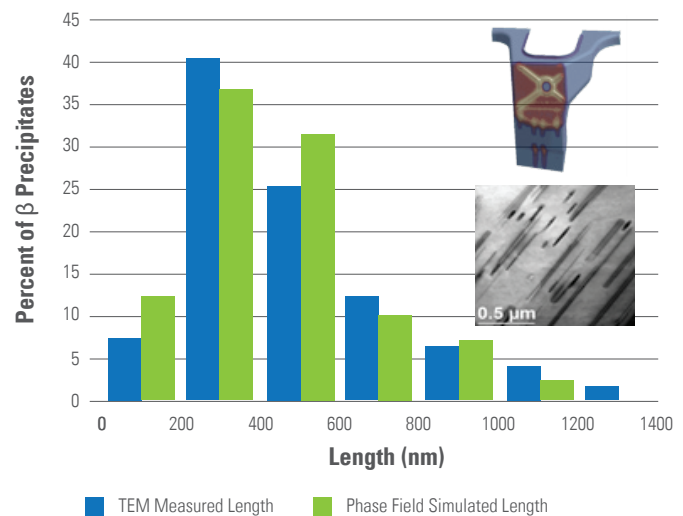


Figure 1. Comparison of calculated and measured length distributions for beta phase precipitates in an AZ91D shock tower die casting (inset) and TEM micrograph.

Magnesium Front-End Research and Development

Developing enabling technologies in a “demonstration structure” for a material capable of 50% weight reduction compared to a steel baseline structure.

United States Automotive Materials Partnership

In 2006, USAMP undertook an extensive study of enabling technologies for incorporation of magnesium-intensive subassemblies in vehicle front-end structures. This effort, collectively entitled “Magnesium Front-End Research and Development,” or MFERD, included (1) an international collaboration engaging researchers from Canada and China; (2) a computer-aided engineering (CAE) study, including vehicle dynamics and crashworthiness; and (3) an inaugural effort in Integrated Computational Materials Engineering of magnesium alloys and processing. The overarching goal of the initiative was to validate the technical prospects for a substantial portion of a vehicle body subassembly to be fabricated from magnesium components, thereby leading to large-scale weight reduction of the body structures by as much as 50% when compared to all-steel counterparts. Prior reporting of the CAE studies confirmed that for at least one candidate structure from an actual production vehicle, weight reduction of 45% could be realized, with concomitant reduction in part count via piece-part integration. In general, massive application of magnesium alloys for achieving vehicle weight reduction targets on this scale will require the ability to integrate many individual piece parts into larger articulated structures using manufacturing technologies of component fabrication, joining, and finishing suitable for mass production.

The focus of the latest phase of this work has been the design, production, and testing of an all-magnesium “demonstration” structure (Figure 1) as a platform for evaluation of critical enabling technologies for component manufacture (e.g., super-vacuum die casting, sheet-forming, and extruding), surface finishing for corrosion protection, and joining. More than 200 such “demonstration” structures were manufactured

by the partnership and were subjected to rigorous testing for durability (e.g., overload and fatigue), as well as corrosion using industry standard cyclic test protocols.

The structures employed two joining technologies (self-piercing rivets and friction-stir linear welding), three distinct surface pretreating processes, and electrophoretic topcoating, which is a standard industrial process. The results demonstrate the feasibility of eventually being able to implement magnesium-intensive design elements in actual vehicle structures.



Figure 1. Friction-stir-welded all-magnesium demonstration subassembly comprised of a central AM60B die casting, AZ31 sheet-formed upper box, and extruded AM30 lower rail.

Establishment of Quality Mapping for Ductility in Magnesium Casting

QM was established and successfully validated in predicting the mean ductility and its statistical variations for an AM60 Mg casting.

Ford Motor Company, University of Michigan, and Pacific Northwest National Laboratory

Magnesium (Mg) castings have found increasing applications in lightweight vehicles because Mg and its alloys are among the lightest structure materials. One critical technical hurdle hindering the wider applications of Mg castings in vehicle applications is its limited ductility. Currently, there is no predictive capability for forecasting ductility as a function of casting geometry. In addition, since the measured ductility typically varies from part to part and from location to location, it is important to consider both the mean value and the statistical variations in ductility prediction to enable lightweighting designs with Mg in ductility-limited applications.

In this work, location-dependent ductility values for a generic component cast under different processing conditions were first obtained through tensile testing. Magmasoft® simulations for each set of processing conditions were then conducted, and the relationships between simulated characteristics and experimentally measured ductility were determined throughout the component. A linear regression technique was next used to predict the local properties of the generic casting and to produce a Quality Map (QM) that indicates the local ductility throughout the generic component, as shown in Figure 1.

Significant statistical variation has also been observed in excised samples for the same locations across different castings. Ductility variations were predicted by considering the variations in the casting process parameters. Qualitatively accurate location-dependent ductility variations have been predicted by incorporating the upper, median, and lower bounds of the filling profiles into the simulation process (see results in Figure 2). Development of accurate simulation techniques, such as the method described here, allows improved prediction of component behavior during the design stage and corresponding optimization of part performance and weight.

Conclusions of this work are as follows: (1) quality mapping for mean ductility was established and successfully validated, and (2) a preliminary method to predict the location-dependent ductility variations for a Mg frame casting has been developed.

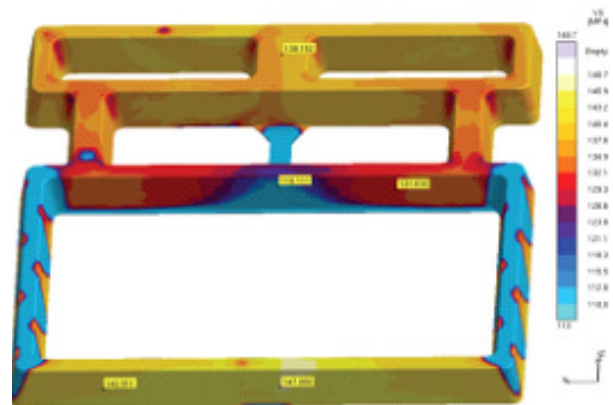


Figure 1. QM for ductility of AM60 casting.

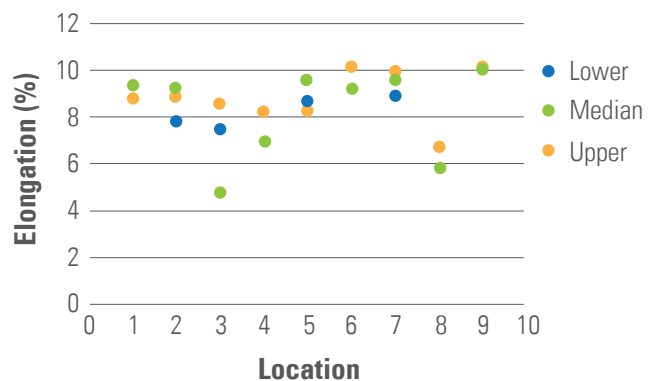


Figure 2. Predicted location-dependent ductility variations in a Mg frame casting based on variations in filling profiles.

Non-Rare Earth Containing Wrought Magnesium Development

Developing a reduced cost method for manufacturing Mg sheet product from wrought feedstock material.

Pacific Northwest National Laboratory

Magnesium (Mg) has the potential to reduce the mass of automobile components by more than 50% over conventional steel, resulting in reduced greenhouse gas emissions and substantial improvement in fuel economy.

The primary goal of this activity was to determine if Mg, when processed in novel ways, can exhibit energy absorption like that of aluminum, thereby expanding the use of Mg for vehicle lightweighting. Earlier work using non-conventional processing was used to develop high strength and ductility in rare-earth (RE) containing Mg alloys. In this project, materials produced with fine microstructure were used as feedstock for extrusion. The extrusions were then used for energy absorption tests using the sample in Figure 1.

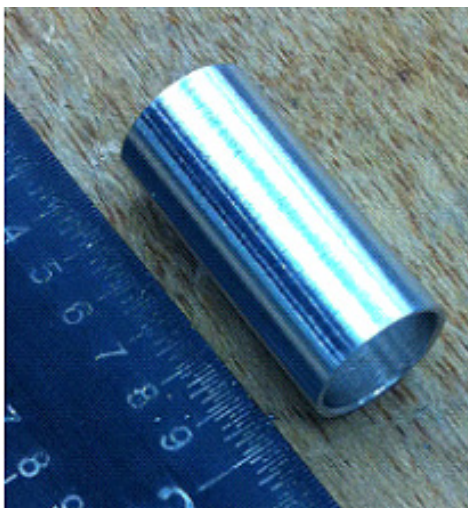


Figure 1. Mg alloy tubular sample used to evaluate energy absorption capacity in a compression test.

The current activity initially showed that the RE containing Mg alloy could exceed the energy absorption of aluminum alloy 6061; using the same processing,

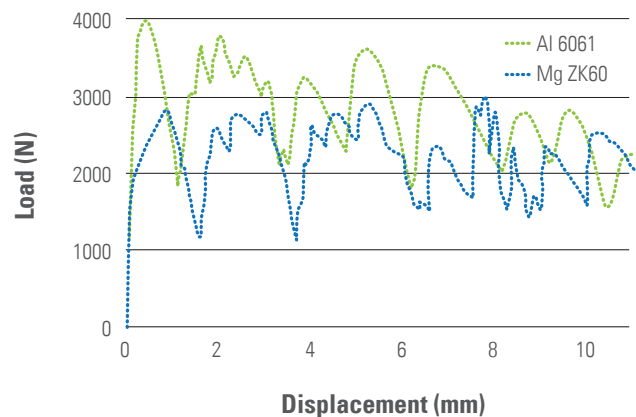


Figure 2. Energy absorption results for aluminum alloy Al6061 and Mg alloy ZK60A showing similar levels.

it showed that this could be achieved by the non-RE containing ZK60A Mg alloy. In fact, the ZK60A samples achieved the same energy absorption at a mass savings of 20% over 6061, as shown in Figure 2.

This energy savings was achieved by producing the ZK60A with a very fine grain size that, in Mg, increases the compressive strength and ductility dramatically. For the initial studies, the processing used is unlikely to be cost-effective for the automotive market; therefore, the project is now focused on developing processing methods to produce very fine grain size in Mg cost effectively. Process development has been using a combination of inverse process modeling, crystal plasticity, and experimental methods to “engineer” the ideal low-cost process.

Advanced Plasma Oxidation

Lowering the cost of carbon fiber conversion by reducing the time needed for the oxidation phase utilizing atmospheric pressure plasma technology.

Oak Ridge National Laboratory and ReMaxCo Technologies

ORNL is leading research and development efforts in lightweight materials for transportation, with a focus on lower-cost carbon fiber, which would be available at a target price of \$5–\$7 per pound.

Significant weight reduction of the vehicle with resulting increases in fuel economy can be achieved by replacing dense materials (such as metals) with strong, lightweight composite materials. Carbon fiber-reinforced composites are excellent candidates for this lightweight material.

Carbon fibers with the properties needed for automotive applications currently sell for \$8–\$15 per pound. The most significant component of carbon fiber composite cost is the cost of the carbon fiber itself; about half of that cost is converting the precursor (starting material) into finished carbon fiber. About half of the conversion cost is in the first step, oxidation.

Recent efforts by the research team consisting of scientists and engineers from ORNL and ReMaxCo have developed a technology that yields a dramatic decrease in the oxidative stabilization time. Oxidative stabilization is two processes occurring simultaneously where the polymer fiber is cross-linked and oxygen is diffused into the fiber. The new plasma-based processing technique, Close Proximity Indirect Exposure, was highly successful and is being scaled-up for continuous processing. The process has been optimized to the point that aerospace-grade polyacrylonitrile (PAN) precursor fiber can be oxidized in an average of 20–30 minutes, and textile-grade (low-cost) PAN can be oxidized in an average of 30–40 minutes compared to the conventional process, which requires 80–120 minutes. Thus, the oxidation time has been reduced by up to 85% compared to that of the conventional oxidative stabilization time, depending upon precursor.

Once carbonized, the fibers yield mechanical properties exceeding the DOE program requirements. Figure 1 shows one of these properties, the tensile strength of carbon fiber, and illustrates the differences between the previous and newly developed methods. Patent applications have been filed covering this area.

Preliminary contact has been established with various equipment manufacturers that could manufacture ovens for the carbon industry based on the new technology. Further information is available in the 2012 DOE Merit Review presentation for this work (Advanced Oxidation & Stabilization of PAN-Based Carbon Precursor Fibers – LM006).

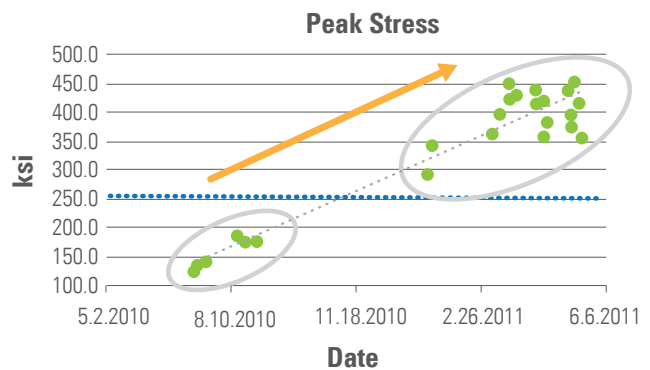


Figure 1. Plot of carbon fiber tensile strength of samples over time. The two groups of samples represent two different methods, as discussed in the text. The dashed line is the DOE programmatic target for the automotive industry. Similar results were seen with the modulus of the carbon fiber.

Vehicle Systems and Analysis



New Air Conditioning Model Validated and Released

NREL's new MATLAB/Simulink CoolSim plug-in air conditioning model was validated to within 2.7% of experimental data and released for public download.

National Renewable Energy Laboratory

When operated, the air conditioning (A/C) system is the largest auxiliary load on a conventional vehicle. A/C loads can account for more than 5% of fuel used annually for light-duty vehicles in the United States. A/C loads can also have a significant impact on EV, PHEV, and HEV performance.

NREL has developed CoolSim, a new air conditioning model written in the MATLAB (matrix library)/Simulink environment to assist heating, ventilation, and air conditioning (HVAC) engineers design improved systems, and to add A/C modeling capability to Autonomie. It runs as both a standalone model or integrated with Autonomie.

CoolSim is a transient model of the A/C system, which includes the compressor, condenser, expansion device, evaporator, and refrigerant lines. It uses a one-dimensional finite-volume formulation of the continuity, momentum, and energy equations to solve the refrigerant thermodynamic and heat transfer performance. Figure 1 shows the Simulink block diagram with system components labeled.

In collaborating with Visteon, NREL validated the CoolSim using 22 test bench data points. For all 22 steady state data points provided by Visteon, the model mass flow rate, condenser, evaporator, and air outlet temperature were all within 2.7% of measured data or closer. Figure 2 shows the comparison of test data to simulation results for the evaporator heat transfer for all 22 data points, and

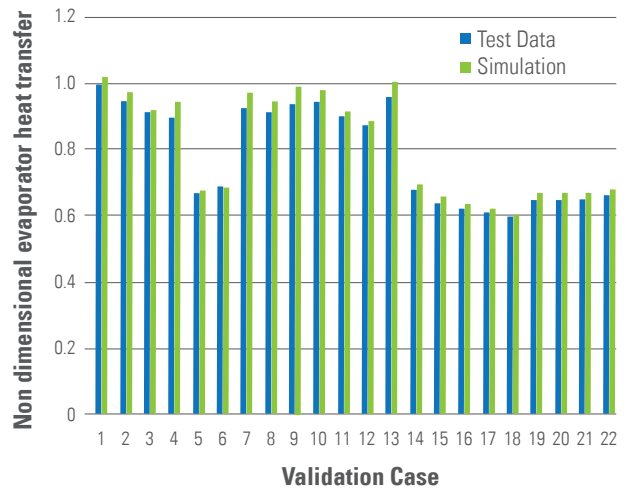


Figure 2. Evaporator heat transfer validation.

also illustrates the accuracy of the model.

The model was also co-simulated in Autonomie using a default mid-sized automobile over the SC03 drive cycle. The results show a 14.7% increase in fuel consumption with A/C on.

A standalone version of the A/C model was released. Autonomie with an integrated CoolSim model will be released in 2013.

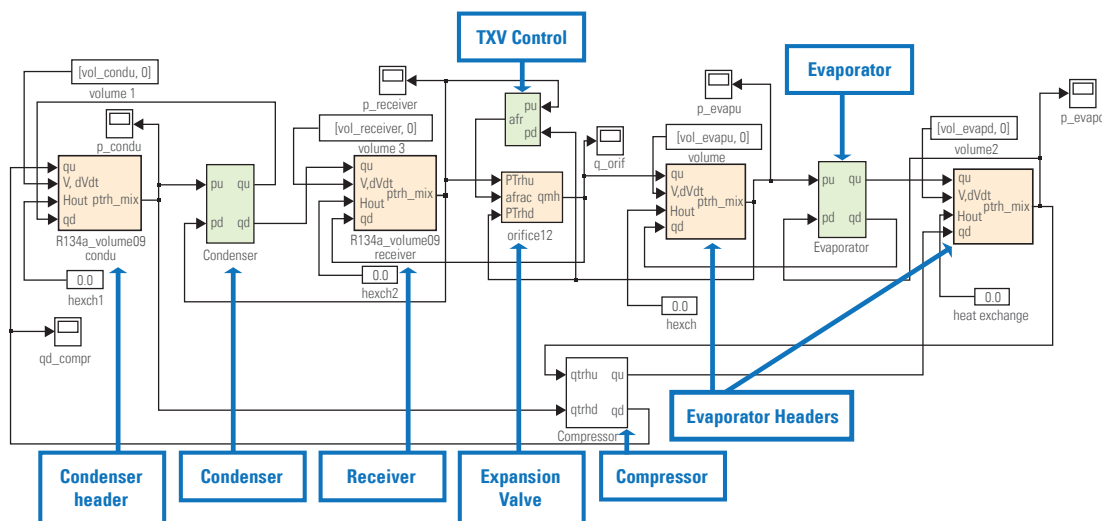


Figure 1. Simulink block diagram of A/C system model.

Accelerating EV Development with New Test Standards

Using state-of-the-art equipment and vehicles, newly developed EV test methods cut testing time by as much as 80%.

Argonne National Laboratory

New EVs coming to market have the benefit of superior range compared with previous-generation technology. However, completing a single test of these new long-range EVs could take as long as 16 hours of uninterrupted driving. The existing test procedure (SAE J1634) was a barrier to development time that could be updated with careful study and testing.

Engineers at ANL have developed new procedures that will greatly reduce the costs and time associated with testing and development that will benefit manufacturers of EVs.

The Society of Automotive Engineers (SAE) organizes hundreds of standard committees that are made up of volunteer engineers from the automotive industry and government. ANL engineers have actively participated in developing and improving standards related to advanced vehicle development since 1993. ANL staff recently chaired the committee to update the plug-in hybrid test procedure (now used to evaluate vehicles like the Chevy Volt). ANL served as co-chair of the EV testing task force and provided key inputs and testing validation for the revision to the standard. A national laboratory is in a unique position to provide unbiased test results and arbitration among all the proposed testing approaches to find the most accurate procedure for the standard. Several original equipment manufacturers and prototype EVs were tested at ANL in order to find the most efficient approaches and reduce any sources of imprecision. The consensus approach was developed, validated at ANL, and successfully balloted by the SAE committee (October 2012).

The new approach allows multiple test cycles (for example, the city and highway cycles) to be run on the same test

day. The efficiency of each cycle is found, and the range for each cycle is carefully calculated. Two test days are now shortened to a single four hour test. Updated range calculations were found to be more repeatable and robust. Figure 1 shows vehicles on a chassis dynamometer, the procedure sequence, and the equations used to calculate range and efficiency.

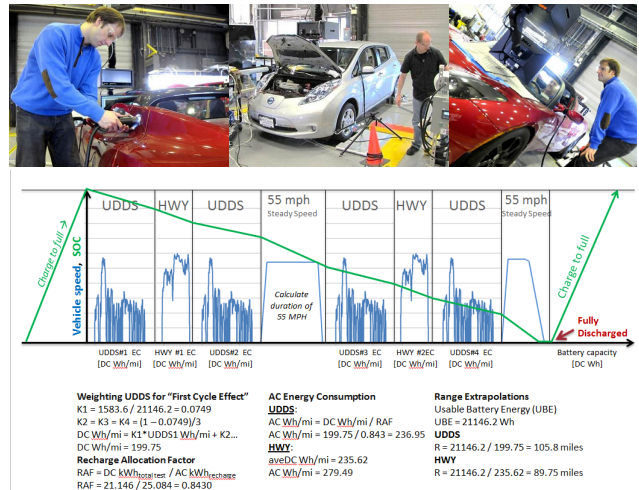


Figure 1. New test procedure will dramatically cut testing time and provide more repeatable results for EVs.

Vehicle Mass: Road Load and Energy Consumption Impact

Energy consumption decrease of up to 4% to 5% for a 10% vehicle mass reduction was quantified for three vehicle powertrain architectures: Internal Combustion Engine, Hybrid Electric, and Battery All-Electric.

Idaho National Laboratory, Oak Ridge National Laboratory, and ECOTality North America

In support of DOE’s and the Vehicle Systems and Analysis Technical Team’s testing and data collection requirements, INL, ANL, ECOTality North America, and DOE’s Advanced Vehicle Testing Activity tested advanced technology vehicles in on-road fleets, test tracks, and laboratory settings in order to determine the real-world petroleum reduction potential of various advanced vehicle technologies.

The impact of vehicle mass on road load force and energy consumption for three vehicle powertrain architectures was measured through test-track coastdown testing and chassis dynamometer testing. Testing was conducted on a Ford Fusion V6 internal combustion engine (ICE) vehicle, a Ford Fusion HEV, and a Nissan Leaf battery electric vehicle (BEV). Testing was conducted at multiple 250-pound test weights for each vehicle. This study provides results for research, development, and modeling efforts.

Coastdown testing quantified the impact of vehicle mass on road load force to be a non-linear trend with respect to change in mass. For a 5% increase in mass, the road load force increases approximately 3%, but for a 5% decrease in mass, the road load force decreases approximately 5%. This trend appears to be consistent across the three powertrain architectures (BEV, HEV, or ICE).

Chassis dynamometer testing quantified the impact of vehicle mass on energy consumption. The largest impact of vehicle mass occurs during “stop and go” city

and aggressive driving. For a 10% reduction in mass, an approximate 4%—5% decrease in percent energy consumption was measured across all powertrain architectures. The conventional vehicle (ICE) has the largest decrease in energy consumption (up to approximately 0.4L/100 km) during aggressive driving due to the inherently lower powertrain efficiency, as compared to HEV or BEV.

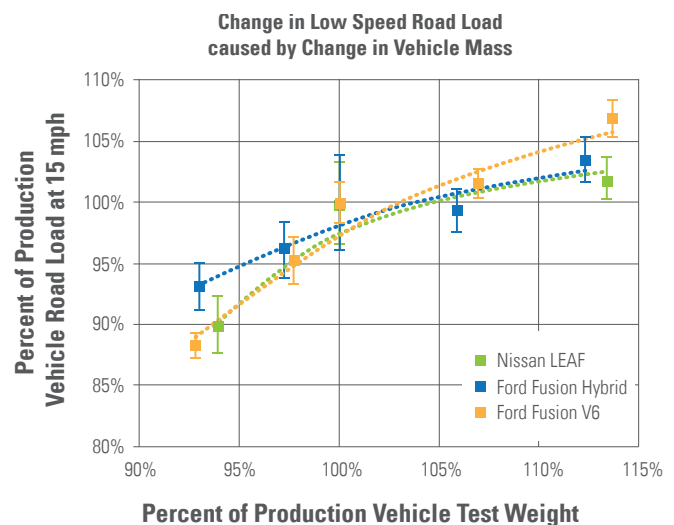


Figure 1. Vehicle Road Load vs. Vehicle Weight with respect to base vehicle

For a 10 % Reduction in Vehicle Mass						
Driving Type	Percent consumption reduction [%]			Energy consumption reduction [Lge/100 km]		
	City	Highway	Aggressive	City	Highway	Aggressive
Conv. V6	~3.5 %	~3.0%	~4.5 %	~0.35	~0.19	~0.40
HEV	~2.5 %	~1.5 %	~4.0 %	~0.12	~0.06	~0.19
BEV	~5.0 %	~0.1 %	~2.5 %	~0.08	~0.01	~0.10

Table 1. Energy consumption reduction achieved after decreasing vehicle mass 10%.

Wireless Power Transfer: Stationary Charging

Wireless power transfer stationary charging development at ORNL achieves 7 kW power charging of plug-in electric test vehicles over 15 cm air gap at greater than 90% efficiency.

Oak Ridge National Laboratory

Wireless charging of plug-in electric vehicles is a safe, convenient, and flexible alternative to conductive charging. ORNL's approach is to develop wireless power transfer (WPT) for autonomous operation, maximizing customer convenience with minimal added components.

ORNL's stationary wireless charging activity is focused on safety (electrical and magnetic fields) and driving international standards development.

Rectified utility voltage is regulated to coarse direct current rail voltage (U_{dc}) level for power control, plus pulse width modulation ratio (d) for cycle-by-cycle control, and overall frequency (ω) to track load and working gap (z) variations. Figure 1 illustrates the main elements of WPT.

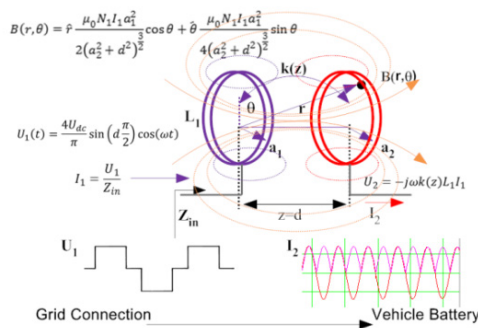
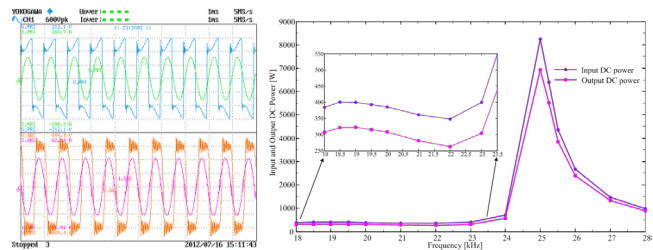


Figure 1. Essential elements of WPT vehicle charging.

ORNL coupling coils are designed using Litz cable for minimum conduction loss at high frequency, and use segmented ferrite back planes (wedges or blocks) to maximize coupling coefficient, $k(z)$ and minimize fringe and back field leakage.

ORNL's primary-side regulated WPT system was tested on an Equinox PHEV and demonstrated in July 2012. Testing was done over a 15 cm gap at 7 kW power level to a vehicle 288V nominal nickel-metal-hydride (NiMH) battery pack at an operating frequency of 25 kHz.

Figures 2 and 3 show the power transfer, input to battery terminals, and measured voltage, and current waveforms.



Figures 2 and 3. Input and output power versus operating frequency at 7 kW power into NiMH battery.

Figure 4 shows magnetic field measurements made 0.8 m from the primary center beneath a car at 8 kW power in and $d=140$ mm.

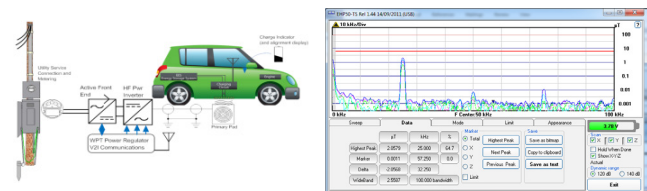


Figure 4. WPT field measurement and validation using Narda EHP-50 E&H Field Analyzer (field at rocker panel is $\sim 2\mu\text{T}$ at 25 kHz).

The program demonstrated 7 kW charging with a near-term goal of scaling power levels to 10 kW and higher.

Interoperability is essential and covers common mounting location on the vehicle, single center frequency (20 kHz or 48 kHz), communications protocol and message set definition, misalignment tolerance and alignment sensing methods, and field measurement and validation for installation certification.

CROSSCUTTING TECHNOLOGIES

Codes and Standards



Optimizing Materials Testing for Hydrogen Service

Improvement in the balance between the test duration and data reliability for hydrogen embrittlement qualification can accelerate material screening and technology deployment.

Sandia National Laboratories

Research by SNL on hydrogen embrittlement testing resulted in a significant modification to existing test procedures that would reduce the test duration without compromising data quality. The current procedures for qualifying metallic materials in compressed hydrogen pressure vessels, according to the American Society for Mechanical Engineers (ASME) code, can require several months to complete. The proposed modified procedures could reduce the time for materials qualification by more than 50%, reducing the effort and cost for screening and deploying material for hydrogen fuel technology.

The well-known phenomenon of hydrogen embrittlement in metals can compromise the structural integrity of hydrogen containment components, raising the possibility of an unintended hydrogen release. The traditional materials test method for hydrogen embrittlement in the ASME code is measuring the fatigue crack growth rate in hydrogen gas. This test method involves subjecting the material to cyclic stresses at a frequency of 0.1 Hz, and measuring the crack growth response. However, measuring the crack growth rate over a sufficient spectrum of stress conditions at 0.1 Hz can be impractical, requiring many weeks for a single test specimen to be qualified.

Through research conducted in its unique Hydrogen Effects on Materials Laboratory, SNL has proposed a modified version of the ASME test method. In this modification, a baseline crack growth rate versus stress relationship is measured at a high frequency, such as 10 Hz. Based on these data trends, further crack growth rate measurements are conducted as a function of frequency at selected stress values. These latter measurements are then employed to correct the

baseline relationship (see Figure 1). In this way, the corrected relationship represents reliable, upper-bound data, but the modified procedures can be executed in a relatively short time period.

SNL is finalizing the modified procedures with a complete validation data set for a range of hydrogen gas pressures and materials. In parallel, SNL has initiated discussions with ASME to ensure the modified procedures can be accepted into the code. SNL has also been active in incorporating its testing knowledge into the CHMC 1 (Compressed Hydrogen Material Compatibility 1) and Society of Automotive Engineers J2579 Standards.

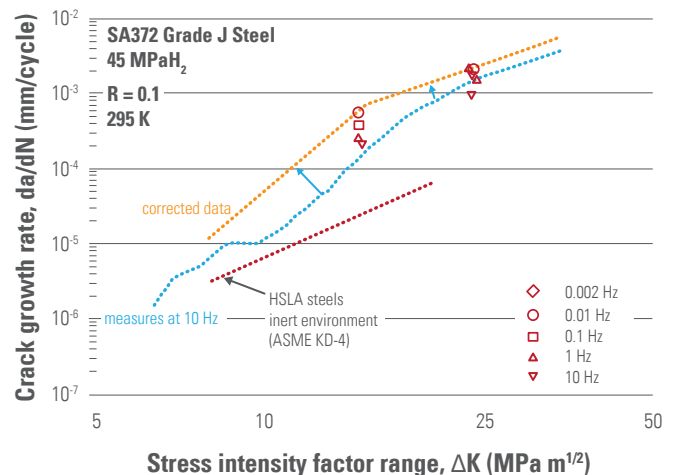


Figure 1. Crack growth rate measurements for a typical pressure vessel steel in hydrogen gas, demonstrating modified procedures for qualifying materials, according to the ASME code.

Publication of Harmonized SAE J2719 Hydrogen Fuel Quality for Fuel Cell Vehicles

Harmonized fuel quality standards promote world wide deployment of fuel cell vehicles.

Department of Energy

The Society of Automotive Engineers (SAE) published SAE J2719 as a final standard on September 20, 2011. This standard was fully harmonized with ISO 14687-2, "Hydrogen fuel—product specification—Part 2: Proton Exchange Membrane (PEM) Fuel Cell Applications for Road Vehicles," which was published November 30, 2012 as an international standard. Full harmonization means that the two standards contain essentially the same list of contaminants and contaminant concentration limits. These standards will be used in many of the key locations where hydrogen fuel cell vehicles are being or will be deployed. The benefits of harmonizing these standards is that the hydrogen supply industry will have one common set of fuel quality requirements with which it must comply, and automotive OEMs can count on consistent hydrogen fuel quality across all of their global markets. The promulgation of SAE J2719 also means that deployment of hydrogen fuel cell vehicles and the associated infrastructure can proceed in the United States. The State of California will enforce SAE J2719 as a requirement for the sale of hydrogen as a retail fuel in the state.

DOE supported this effort in several ways, including:

- Supporting work of the Chairman of the SAE Fuel Cell Technical Committee, who was instrumental in advancing SAE J2719 through the development and promulgation processes.
- Generating data required to develop Table 1 in the SAE J2719 Standard, copied on the right. This data generation effort included testing at several laboratories and at the NREL Wind Site.
- Validation of the ASTM laboratory test methods, referenced in the SAE J2719 standard, to determine the concentration of contaminants in a hydrogen sample.

The following national laboratories and universities participated in the experimental testing that serves as the basis for this standard (in alphabetical order):

- Argonne National Laboratory
- Clemson University
- Hawaii Natural Energy Institute/University of Hawaii
- Los Alamos National Laboratory
- National Institute of Standards and Technology
- National Renewable Energy Laboratory
- Savannah River National Laboratory
- University of Connecticut
- University of South Carolina

TABLE 1 - HYDROGEN FUEL QUALITY SPECIFICATION GUIDELINE

- Units are $\mu\text{mol/mol}$ unless otherwise specified
- All limits are subject to revision after additional testing under operational conditions and improved standardized analytical procedures
- Limits are upper limits except for the hydrogen fuel index which is a lower limit.
- Gaseous sampling uses procedures in ASTM D7606-11

Constituent	Chemical Formula	Limits	Laboratory Test Methods to Consider and Under Development ^e	Minimum Analytical Detection Limit
Hydrogen fuel index	H ₂	> 99.97%		
Total allowable non-hydrogen, non-helium, non-particulate constituents listed below		100		
Acceptable limit of each individual constituent				
Water ^a	H ₂ O	5	ASTM D7653-10, ASTM D7649-10	0.5
Total hydrocarbons ^b (C ₁ basis)		2	No standardized test method available ASTM D 1946 under revision (Work Item 22378)	0.1
Oxygen	O ₂	5	ASTM D7649-10	1
Helium		300	ASTM D1945-03	10
Nitrogen, Argon	N ₂ , Ar	100	ASTM D7649-10	60
Carbon dioxide	CO ₂	2	ASTM D7649-10, ASTM D7653-10	0.1
Carbon monoxide	CO	0.2	ASTM D7653-10	0.2
Total sulfur ^c		0.004	ASTM D7652-11	0.004
Formaldehyde	HCHO	0.01	ASTM D7653-10	0.01
Formic acid	HCOOH	0.2	ASTM D7550-09, ASTM D7653-10	0.2
Ammonia	NH ₃	0.1	ASTM D7653-10	0.1
Total halogenates ^d		0.05	No standardized test method available ASTM developing new standard (Work Item 23815)	0.01
Particulate Concentration		1 mg/kg	ASTM D7650-10, ASTM D7651-10	0,005 mg/kg

- Units are $\mu\text{mol/mol}$ unless otherwise specified
- All limits are subject to revision after additional testing under operational condition
- Limits are upper limits except for the hydrogen fuel index which is a lower limit
- Gaseous sampling uses procedures in ASTM D7606-11

Table 1. Hydrogen Fuel quality specification guideline.

Onboard Hydrogen Storage



Material Requirements for Viable Onboard Hydrogen Storage Using Metal Hydrides

Engineering analyses established that no current metal hydride material can sufficiently meet all minimal performance requirements for reversible onboard storage in light-duty vehicles.

Savannah River National Laboratory, United Technologies Research Center, General Motors, and Pacific Northwest National Laboratory

New integrated system models developed within the Hydrogen Storage Engineering Center of Excellence (HSECoE) can be used to clearly define the material properties necessary for a practical onboard rechargeable metal hydride material (i.e., allows direct refueling with gaseous hydrogen at pressures less than 350 bar) to achieve DOE's 2017 hydrogen storage targets.

By combining storage system and vehicle models, candidate metal hydrides materials integrated into storage vessel designs were screened—over a range of chemical, physical, and geometrical parameters—to determine if they could satisfy the DOE 2017 hydrogen storage performance targets. Minimal balance-of-plant components were assumed for systems with and without a hydrogen combustion loop for supplemental heating to release the hydrogen from the metal hydride material. The system weight and volume were driven by the stringent requirements to achieve a 3.3 minute refueling time.

The resulting assessment performed by the HSECoE indicated that no currently known onboard rechargeable metal hydride can satisfy the necessary requirements for vehicle applications. This is illustrated in Figure 1 by the fact that no currently known hydride materials lie within the green or blue boxes, respectively, which offer both the necessary reaction enthalpies and hydrogen gravimetric storage capacities to achieve the DOE 2017 hydrogen storage targets. The modeling shows that for hydrides and hydride mixtures (i.e., destabilized hydride systems), which have sufficiently low enthalpy so that waste heat from the fuel cell can be used to release the hydrogen, at least an 11 wt.% hydrogen storage hydride material is required. For hydride systems that

have higher hydrogen release enthalpies or require higher temperatures to achieve sufficiently high rates of hydrogen release, even greater hydrogen storage capacity (14 wt.%) is required; this is because some hydrogen will be consumed in a combustion loop. When combustion of some of the stored hydrogen is required for hydrogen release, then the target for 90% onboard efficiency is difficult to meet.

As a result, the HSECoE discontinued work on metal hydrides for vehicle storage systems. This conclusion applies specifically to light-duty vehicles and does not preclude metal hydrides from use in different applications or the future development of hydrides with improved material properties.

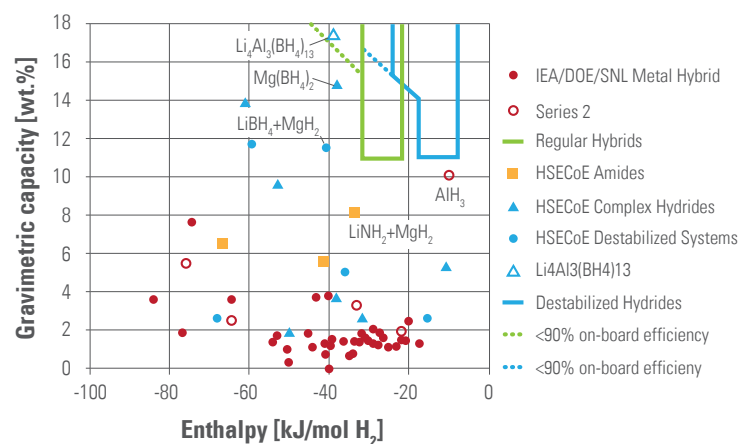


Figure 1. The green and blue windows enclose the regions where systems of regular and destabilized metal hydrides can be designed that satisfy the DOE 2017 targets.

Systematic Analysis and Avoidance of Material-Based Hydrogen Storage System Failure Modes

Adsorbent and chemical hydrogen storage systems were improved through identification of failure modes and prioritization of mitigation actions using the Failure Mode and Effects Analysis technique.

Hydrogen Storage Engineering Center of Excellence

The Hydrogen Storage Engineering Center of Excellence (HSECoE) completed a comprehensive analysis of potential failure modes associated with their modeled adsorbent and chemical hydrogen storage systems. Using a technique from the automotive industry for improving product reliability, called Failure Mode and Effects Analysis (FMEA), the HSECoE partners were able to identify and minimize the key causes of high-risk failure modes for each system. This analysis has led to prototype designs with less risk and a greater probability of successfully achieving the desired system functions.

The HSECoE team recognized FMEA as a tool that can be used to evaluate risk, reduce failure modes, and guide the validation test plan. They used the FMEA methodology (per SAE J1739) to analyze each material-based storage system. The key steps for FMEA include identification of failure modes, along with their severity rating; identification of potential causes, along with their occurrence rating; and documentation of control measures, along with their detection ratings. The functions within FMEA were directly aligned with DOE's system targets, and the effects along with their severity were assessed.

A result of FMEA was the assignment of a Risk Priority Number (RPN)—which is the product of the severity, occurrence, and detection ratings—to each potential failure mode. Establishing the RPN allowed the team to identify the key causes of high-risk failures and develop action items to reduce risk. A total of 96 potential failure modes were identified and analyzed for the adsorbent system, as well as 108 for the chemical hydrogen system. Figure 1 provides a graphical Pareto summary

of the RPN ratings for the chemical hydrogen system FMEA. The relative ranking allowed the team to visualize that there were some failure modes that have higher risk than others. In addition, common risks within each system were identified, such as flocculation and clogging of the chemical hydrogen slurry system.

The team has utilized FMEA as a tool to prioritize potential failure modes and then develop specific action items to reduce the risk in the overall design based on the high RPN failure modes. The potential failure modes and the corresponding RPNs will be reevaluated after component and system prototype testing have been performed.

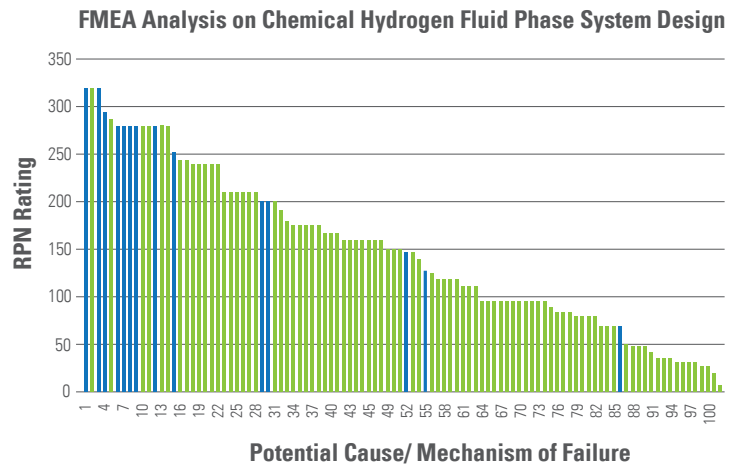


Figure 1. Chemical Hydrogen Storage System FMEA (excludes any RPNs related to material discovery research).

Best Practices Reference Document Released

A reference document was created to improve the characterization of properties for hydrogen storage materials developed by researchers.

H2 Consulting LLC and National Renewable Energy Laboratory

Work has been completed on the “[Recommended Best Practices for the Characterization of Storage Properties of Hydrogen Storage Materials](#)” document.¹ This document, which will serve as a concise reference guide for hydrogen storage researchers, covers the best practice protocols to correctly measure hydrogen storage material properties, including material capacity, kinetics, cycle life, and thermodynamics. By ensuring proper testing and calibration techniques, as well as through error reduction, measurements for hydrogen storage material properties will be significantly more reliable.

The necessity of this effort can be appreciated by comparing the disparity of results in Figure 1 with the close agreement of results in Figure 2. Figure 1 shows the

inconsistent results obtained from a round-robin effort conducted by international researchers. Figure 2 shows the consistent results obtained from a recent round-robin effort led by NREL where it provided the Best Practices document to the laboratories involved to ensure that consistent protocols were used.

This document will centralize the common metrics and best practices for measuring the hydrogen storage properties of new materials that are being developed within the DOE Hydrogen Storage sub-program, as well as enhance the future accuracy, reproducibility, and robustness of hydrogen capacity measurements. The document is also being used as a reference guide to measure material storage capacity of other gases, such as methane and carbon dioxide.

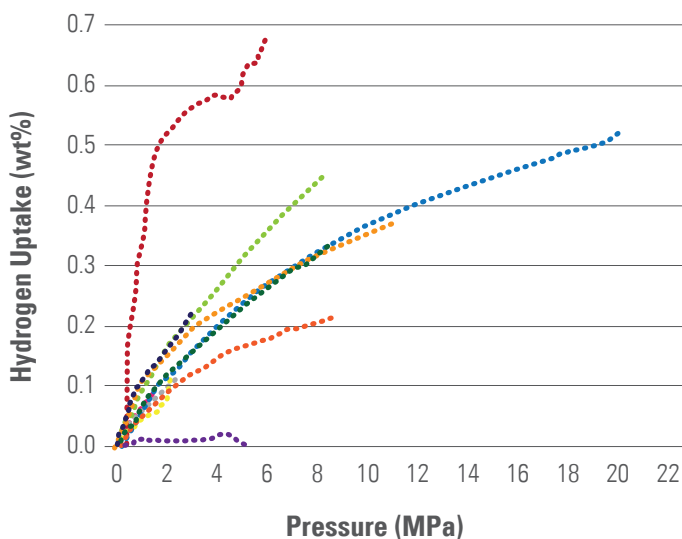


Figure 1. 295 K isotherms taken at multiple laboratories. The inconsistent results emphasize the need for rigorous test protocols to ensure that material properties reported can be interpreted with confidence.²

¹ http://www1.eere.energy.gov/hydrogenandfuelcells/pdfs/best_practices_hydrogen_storage.pdf

² C. Zlotea, P. Moretto, and T. Steriotis. A round-robin characterisation of hydrogen sorption properties of a carbon based material, Intl. J. Hydrogen Energy, 34 (2009) 3044-3057.

³ http://www.hydrogen.energy.gov/pdfs/review12/st014_parilla_2012_o.pdf

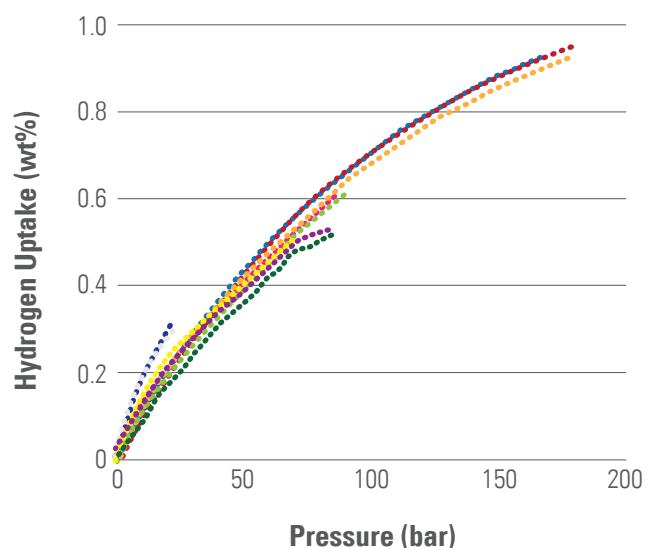


Figure 2. 298 K isotherms taken at multiple laboratories. The close agreement shows the value added from the use of consistent protocols.³

Validation of Hydrogen Storage Using Weak Chemisorption

Hydrogen storage capacity measurements and spectroscopic characterizations across multiple laboratories were used to obtain direct evidence for reversible, room temperature, hydrogen storage using the “spillover” mechanism.

National Renewable Energy Laboratory

An international team led by NREL has demonstrated and provided the first direct spectroscopic evidence of hydrogen storage using the “spillover” mechanism. The results were validated by replication of sample synthesis and evaluation at multiple laboratories.

Hydrogen storage using weak chemisorption (spillover) is expected to reduce system complexity due to its reported ability to store large amounts of hydrogen at room temperature; however, this field of research has been hampered by reproducibility issues. As a result, DOE established an international team led by NREL to develop and perform the requisite measurements in order to establish the validity, capacity, and overall performance of spillover-type materials.

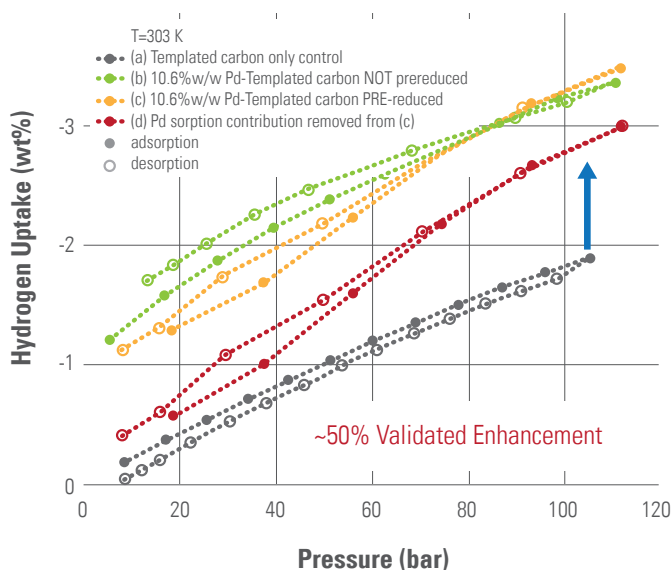


Figure 1. Hydrogen storage capacity measurements of PdTC showing validated 50% enhancement using spillover.

The group systematically examined a series of established spillover-type materials to resolve critical issues surrounding sample reproducibility, lack of spectroscopic evidence, and the ultimate storage capacity achievable using spillover. Three separate laboratories—NREL, Institut de Chimie et des Matériaux, and the University of Hawaii—demonstrated a reproducible room temperature hydrogen sorption enhancement for two separate materials: Pd/Templated Carbon (PdTC) and Ru/BCx. The apparent enhanced hydrogen sorption capacity using spillover is well beyond what is expected for conventional physisorption of molecular hydrogen, as shown in Figure 1. Spectroscopic evidence obtained, including Nuclear Magnetic Resonance (NMR) and Diffuse Reflectance Infrared Fourier Transform Spectroscopy (DRIFTS), as shown in Figure 2, also identifies the reversible room temperature formation of unique hydrogen-carbon (C-H) substrate interactions.

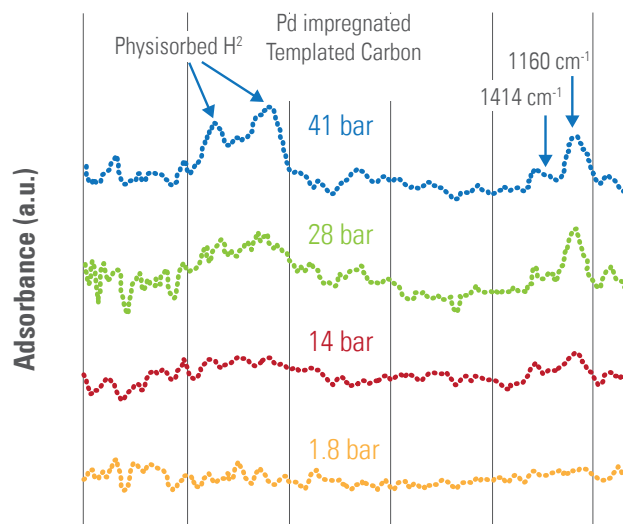


Figure 2. DRIFTS spectra of PdTC following room temperature H_2 charging, where unique reversible C-H peaks are observed between 1,160 and 1,414 cm^{-1} . A similar effect is observed in NMR experiments.

Grid Interaction



Enabling Technologies for Vehicle-Grid Communication

Electronic modules support verification of standard communication protocols between EVs, EV supply equipment, and energy service providers—an enabler for smart charging.

Argonne National Laboratory

Members of the U.S. DRIVE Grid Interaction Technical Team directly support the connectivity and communications committees of SAE providing technical expertise and laboratory resources to aid in the development and verification of technology and proposed standards for connecting EVs (including battery electric and PHEVs), EV supply equipment (EVSE, or charge equipment), and energy service providers (ESPs, e.g., a local utility).

The driver for this activity is EV consumer confidence. EVs should be compatible with any publicly available EVSE and support standard communication protocols to enable smart charging in the future. This requires a standard plug on the charge cord and receptacle on the vehicle (collectively referred to as the charge coupler), as well as a standard method of sending and receiving messages between the EV, EVSE, and ESP.

A standard charge coupler was adopted this year (SAE J1772™), and the standards for messaging and communication protocols are in process (SAE J2836, J2847 and J2931). Adopting a standard requires not only agreement between stakeholders on requirements (i.e., the document to be published), but also verification in laboratory or field testing. Since the hardware necessary to test standard communication between the EV, EVSE, and ESP was not commercially available, ANL utilized the expertise of its Embedded Controls Laboratory and a small electronic component manufacturer to design and fabricate prototype modules for energy measurement and communication (shown in the figures).

These components will be utilized in the EV-Smart Grid Interoperability Centers being set up at ANL and the Joint Research Centre in Europe to develop standard

test procedures for EV-EVSE compatibility and EV-EVSE-ESP interoperability (SAE J2953/ISO 51118).

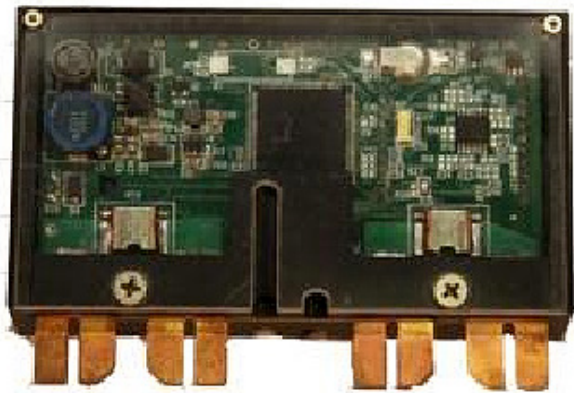


Figure 1. Fourth generation Energy Use Measurement Device; proof-of-concept device to measure and communicate charge energy. The prototype is a fraction of the size and cost of existing smart meters.



Figure 2. Electric Vehicle Communication Controller; Supports development of test methods to evaluate power line communication technologies that enable messaging between EVs, charge equipment, and energy service providers.

FUEL INFRASTRUCTURE TECHNOLOGIES

Fuel Pathway Integration



Well-to-Wheel Analysis

In the modeled scenario, central hydrogen production from biomass gasification with delivery via gas truck or pipeline offers low cost and low greenhouse gas emissions.

Argonne National Laboratory

The Fuel Pathway Integration Technical Team (FPITT) provided a comprehensive review of the analysis methods, assumptions, and data used in the 2012 update of DOE’s techno-economic and well-to-wheels (WTW) analyses. FPITT members identified issues and gaps based on energy industry perspectives. The analysis provided insight on specific gaps, including comparably low levelized costs of hydrogen produced from biomass; variations in stations sizes and analysis periods, resulting in inconsistent comparisons; and unlikely operational logistics for large gas terminals. The 2012 analysis is an update to a 2009 report entitled, *Hydrogen Pathways: Cost, Well-to-Wheels Energy Use, and Emissions for the Current Technology Status of Seven Hydrogen Production, Delivery, and Distribution Scenarios* (NREL/TP-6A1-46612), which is available at <http://www.nrel.gov/docs/fy10osti/46612.pdf>.

The update involved using revised models that are based on 2007 dollars and updated assumptions; using an onboard storage pressure of 10,000 psi (700 bar) with a sensitivity of 5,000 psi (350 bar); adding vehicle costs and vehicle-cycle energy use and emissions; using a FCV penetration of 15%; and analysis of three additional pathway options (hydrogen delivery via gas in trucks, cryo-compressed dispensing, and distributed production via reforming of ethanol).

Figure 1 shows the resulting levelized costs and greenhouse gas emissions for the 10 pathways analyzed. The lowest-cost options are distributed reforming of natural gas and biomass gasification with delivery of liquid hydrogen in trucks. The options with the lowest WTW greenhouse gas emissions are distributed reforming of bioethanol and electrolysis based on wind-generated electricity with pipeline delivery.

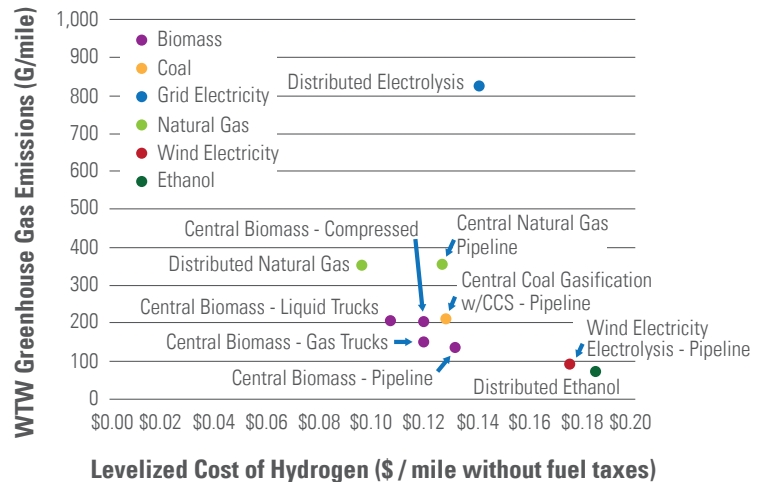


Figure 1. Comparison of hydrogen levelized cost and greenhouse gas emissions between 10 pathways.

Hydrogen Delivery



Increased Tube Trailer Capacity

The addition of a fifth tube leads to an 18% increase in capacity for key hydrogen delivery technology.

Lincoln Composites, Inc.

Safe and affordable transportation of compressed hydrogen gas is vital to the widespread commercialization of FCV. The users of these vehicles will demand convenient access to hydrogen at affordable prices. However, the current hydrogen pipeline infrastructure in the United States is insufficient to meet this demand. To meet the demand for distribution of inexpensive, readily available hydrogen, Lincoln Composites has developed the TITAN™ Module and the TITAN5™ Trailer.

Lincoln Composites' new TITAN5™ Trailer carries 726 kg of hydrogen, exceeding the DOE 2015 target of 700 kg. The trailer, shown in Figure 1, offers a bulk hauling system with an 18% increase in payload capacity relative to its previous TITAN™ modules. The trailer can transport two and a half times the compressed gas payload of steel tube trailers, while maintaining maximum gross vehicle and axle weights comfortably within regulated limits. These innovations, achieved through the use of high-strength composite vessels, represent a greater than 35% reduction in cost. This reduction is in comparison to the 2010 cost estimate of approximately \$930/kg for steel tube trailer technology.

The overall gross vehicle weight of semitrucks pulling the 40-foot TITAN5™ module is below the average steel tube trailer weight of 45 metric tons, even after adding capacity to the existing TITAN™ platform to develop the TITAN5™ trailer. The TITAN5™ trailer uses four of the original 38.5-foot TITAN™ cylinders and incorporates a 28.5-foot-long fifth tank along the bottom channel of the trailer. This additional cylinder results in an overall storage capacity of 8.8 metric tons of compressed natural gas, or 726 kilogram (kg) of compressed hydrogen gas at 250 bar, while only increasing the projected truck/semitrailer mass from 35 to 38 metric tons. This is an 18% increase in hauling capacity relative to the baseline TITAN™ module.

At 726 kg, the hydrogen capacity of the TITAN5™ Trailer exceeds the 2015 goal of 700 kg but remains short of the 2020 goal of 940 kg. Further progress is possible toward the 2020 goal, specifically by increasing the operating pressure of the system. Redesign and requalification of the TITAN™ vessels at higher pressure is currently not feasible given the high qualification costs and uncertainty in industry regarding the required operating pressure. The U.S. DRIVE Hydrogen Team will monitor industry trends in delivery pressures and establish research activities as needed to meet 2020 Partnership Goals.

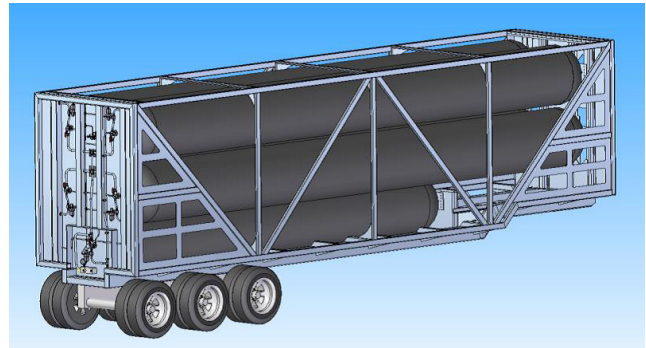


Figure 1. Solid model of TITAN5™ Trailer system with sides and doors removed to show mounting of additional 28.5-foot long TITAN™ tank in keel of trailer.

Hydrogen Production



Improved Hydrogen Evolution in Recombinant Cyanobacteria

Multiple molecular biology techniques were combined to improve enzyme assembly and boost hydrogen evolution activity.

J. Craig Venter Institute

Researchers at the J. Craig Venter Institute (JCVI) have demonstrated dramatic improvements in the hydrogen evolution activity of recombinant *Synechococcus elongatus* cyanobacteria using a non-native, oxygen-tolerant hydrogenase enzyme, raising the activity to 35 nmole H₂/mg protein/hr, a 20-fold increase over the original recombinant strain. Oxygen sensitivity is the main barrier to continuous photolytic biological hydrogen production. Insertion of a more oxygen-tolerant hydrogenase into cyanobacteria with subsequent improvements to hydrogen evolution activity is a step toward meeting DOE's long-term goal of continuous hydrogen production for eight hours.

Some cyanobacteria produce hydrogen naturally at low levels and can be farmed using land and water that are unsuitable for food crops. The ease of genetic manipulation makes them even more useful for biofuel production. However, low-cost hydrogen from solar-driven water splitting is limited by the hydrogenase enzyme's oxygen sensitivity, which shuts down production after approximately two minutes.

To address the oxygen sensitivity, the researchers inserted an oxygen-tolerant hydrogenase gene into the *Synechococcus elongatus* genome. Rather than choosing from the small number of characterized hydrogenases, a gene from a set of DNA sequences isolated in a JCVI ocean sampling project (a nearly identical gene was later found in a deep-ocean strain of the bacteria *Alteromonas macleodii*) was selected and shown to be unusually stable in oxygen. However, the recombinant strain had low hydrogen production.

To improve the hydrogenase enzyme activity, they altered parts of its protein that act as a "molecular wire,"

shuttling electrons to the catalytic center of the enzyme. These changes improved hydrogen evolution by the recombinant cyanobacteria five-fold over the unimproved strain. To give the cells the tools to assemble the active form of the non-native hydrogenase enzyme, the team also added maturation genes from *Alteromonas macleodii* to the cyanobacteria's genome. Inserting additional promoters (sequences that control when genes are turned on) increased hydrogen evolution activity four-fold. When combined, the modifications increased hydrogen evolution 20-fold.

In the future, JCVI will continue to refine the enzyme activity and maturation gene expression, as well as improve the connection of the enzyme with *Synechococcus elongatus*'s energy pathways, with a goal of increasing activity 100-fold by 2014.

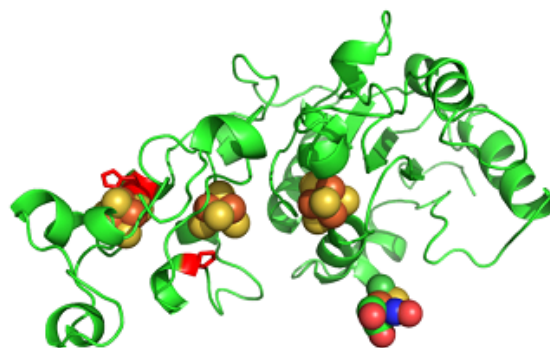


Figure 1. A model of the hydrogenase enzyme showing the small subunit protein (green ribbons) and metal clusters (colored spheres). The two amino acids in red were altered by the researchers.

Updates to the Hydrogen Production Analysis Model

Critical updates maintain the efficacy of a key analytical tool.

National Renewable Energy Laboratory

The newly updated Hydrogen Production Analysis Model (H2A) Version 3 provides DOE's Fuel Cell Technologies Program with an important, technology-neutral cost calculator for developing cost targets for hydrogen production technologies. With the H2A model, DOE can assess progress toward its goals for various hydrogen production technologies under development. Similarly, researchers are able to compare process options to identify key challenges and cost-reduction opportunities. In both cases, the H2A model can help to focus limited resources. In order to keep the model relevant, periodic updates are needed to incorporate new knowledge and re-evaluate assumptions.

Within the last year, significant changes have been made to H2A, ensuring that the detailed technical and economic assumptions within the model are up to date. The first step in the process was a revision to the templates for central and forecourt hydrogen production methods. This included making structural changes to the model, developing strategies for updating cost values, revising common tables, and reviewing common assumptions, such as cost of land. Updated assumptions (e.g., for feedstock costs and plant design specifications) for the Central Production (long term, greater than 50,000 kg/day) template were developed. In addition, all dollar amounts were converted from 2005 dollars to 2007 dollars, and the baselines for feedstock and utility price projections are now based on 2009 Annual Energy Outlook (AEO) Reference Case data. The Forecourt Production (near term, 1,500 kg/day) template required several additional updates, including an in-depth review of "Nth plant" assumptions and input from the Delivery sub-program regarding compression, storage, and dispensing costs. See Figure 1 for a more complete list.

After the model was updated, the template changes were tested, and updated assumptions and approaches underwent a thorough review with stakeholders from industry and DOE.

H2A Version 3 has been a key resource in publishing DOE's updated Multi-Year Research, Development, and Demonstration Plan, as well as the Production sub-program's technology cost threshold analysis. By applying a common methodology to each technology in the production portfolio, an equitable evaluation of technologies can be made and appropriate targets developed.

http://www.hydrogen.energy.gov/h2a_production.html

Capital Costs (updated to 2007\$)	Plant Design Specifications (e.g., size, capacity factor)
Feedstock Costs (AEO 2009 Reference Case)	Cost of Land (increased from \$5k to \$50k/acre for urban land)
Financial Assumption (e.g., IRR, tax rate)	Construction Period (increased from 2 to 3 years)
Operating Costs/Other (labor and other costs updated)	In-Depth Review of Nth Plant and Resulting Cost Assumptions

Table 1. Examples of updates to H2A Version 3.

